Final Research Report
Research Project T9903, Task 12
Item No. 205
Microzonation for Wind Engineering

MICROZONATION FOR TEMPERATURE AND WIND FOR THE STATE OF WASHINGTON

by

Shila Kappayil
Graduate Research Assistant

Dorothy Reed
Professor of Civil Engineering

Washington State Transportation Center (TRAC)
University of Washington, Box 354802
University District Building
1107 NE 45th Street, Suite 535
Seattle, Washington 98105-4631

Washington State Department of Transportation
Technical Monitor
E. H. Henley
Bridge Engineer

Prepared for

Washington State Transportation Commission
Department of Transportation
and in cooperation with
U.S. Department of Transportation
Federal Highway Administration

September 1996

TECHNICAL REPORT STANDARD TITLE PAGE

1. REPORT NO.	2. GOVERNMENT ACCESSION NO.	3. RECIPIENT'S CATALOG NO.
WA-RD 402.1		

4. TITLE AND SUBTITLE	5. REPORT DATE
MICROZONATION FOR TEMPERATURE AND WIND FOR THE STATE OF WASHINGTON	September 1996
	6. PERFORMING ORGANIZATION CODE
7. AUTHOR(S)	8. PERFORMING ORGANIZATION REPORT NO.
Shila Kappayil and Dorothy Reed	
9. PERFORMING ORGANIZATION NAME AND ADDRESS	10. WORK UNIT NO.
Washington State Transportation Center (TRAC) University of Washington, JD-10 University District Building; 1107 NE 45th Street, Suite 535 Seattle, Washington 98105-4631	11. CONTRACT OR GRANT NO. Agreement T9903, Task 12
12. SPONSORING AGENCY NAME AND ADDRESS	13. TYPE OF REPORT AND PERIOD COVERED
Washington State Department of Transportation Transportation Building, MS 7370 Olympia, Washington 98504-7370	Final research report
	14. SPONSORING AGENCY CODE

15. SUPPLEMENTARY NOTES

This study was conducted in cooperation with the U.S. Department of Transportation, Federal Highway Administration.

16. ABSTRACT

Temperature and wind are the major microclimate parameters that were considered the microzonation of Washington State. Thermal movements associated with bridges and wind pressure loadings for traffic signs, signals, and luminaires are major concerns in Washington. Air temperature data for 49 stations across the state were obtained and were converted to the corresponding composite bridge temperature values. Maps of maximum, minimum, and range of air and bridge temperatures were created to identify the temperature pattern of the state and also to develop an isothermal map of mean bridge temperature ranges. Wind microclimate study included an investigation into incorporating a three-second gust wind into the AASHTO standards for calculating wind pressure on structural supports of traffic signs, signals, and luminaires. The new value of Ch (boundary layer profile factor), the primary parameter that changes when using a 3-second gust, were obtained by comparing the velocity profiles for the hourly, fastest-mile, and 3-second gust wind speeds. Adjustment of the gust factor is also included.

17. KEY WORDS	18. DISTRIBUTION STATEMENT
temperature, wind loadings, bridge structural design	No restrictions. This document is available to the public through the National Technical Information Service, Springfield, VA 22616

19. SECURITY CLASSIF. (of this report)	20. SECURITY CLASSIF. (of this page)	21. NO. OF PAGES	22. PRICE
None	None	90	

DISCLAIMER

The contents of this report reflect the views of the authors, who are responsible for the facts and the accuracy of the data presented herein. The contents do not necessarily reflect the official views or policies of the Washington State Transportation Commission, Department of Transportation, or the Federal Highway Administration. This report does not constitute a standard, specification, or regulation.

TABLE OF CONTENTS

LIST OF FIGURES

LIST OF TABLES

EXECUTIVE SUMMARY

Microzonation may be defined as the characterization of the microclimate for a given region. Temperature and wind are the major microclimate parameters that are considered for structural engineering design in the state of Washington. Thermal movements associated with bridges and wind pressure loading for traffic signs, signals, and luminaires are major concerns in Washington. Therefore, a study of the extreme temperature and wind patterns in Washington State was undertaken to map isotherms and modify wind pressure equations to provide more accurate design information. This investigation was separated into two parts: temperature and wind.

Current AASHTO specifications for the design of composite bridges do not consider the microclimate differences within the state of Washington. Therefore, an isothermal map of effective bridge temperature ranges was developed using a computer software program called MapInfo. Temperature data from 49 stations across Washington State were obtained and analyzed to compute bridge temperatures using a method outlined in research conducted by Moorty [2]. Maps were created for the maximum, minimum, and range of air and bridge temperatures, respectively. These maps will be useful in identifying the temperature patterns of Washington State and in accurately predicting the temperature movements of composite bridges.

The bridge temperature range map shows that more than half of the stations under consideration fall outside of the temperature ranges recommended by AASHTO. It also reveals that majority of the stations falling below this range are in the western half of the state. Therefore, in this region, thermal movements could be over-estimated if the AASHTO values are used. By using the isothermal map developed in this project with the AASHTO specification, WSDOT can avoid unnecessary costs associated with the over-estimation of the bridge movements.

For the wind microclimate study, data from seven stations across Washington State were obtained and analyzed. This part of the project also included an investigation into incorporating a 3-second gust wind speed into the AASHTO standards for calculating wind pressure on the structural supports of traffic signs, signals, and luminaires. The present AASHTO specification (1994) is based upon a fastest-mile wind speed; therefore, the substitution of the new 3-second gust, consistent with the proposed 1995 ASCE standard, would require an adjustment of other design parameters. This investigation of parameter variation for the new wind speed was undertaken for the AASHTO specification.

The primary parameter that changes when the pressure equation employs a new wind speed is the representation of the boundary layer profile. The adjustment of the representation can be obtained through the adjustment of the boundary layer profile factor C_h. The factor C_h is also known as the coefficient for height above ground in the AASHTO specification. In order to obtain the adjusted C_h values corresponding to the 3-second gust, the atmospheric boundary layer velocity profiles for the hourly, fastest-mile, and 3-second gust wind speeds were calculated and compared. A gust factor of unity was found to be appropriate for use with the 3-second gust wind. The ratios of the proposed (new) and the existing (old) AASHTO equations for the calculation of pressure were also obtained. The values of C_hn/C_ho (ratio of new C_h to the old C_h) obtained from the velocity profiles and from the comparison of the new and old equations were reasonably close. Further investigation of the drag coefficient was recommended for better results.

INTRODUCTION AND RESEARCH APPROACH

THE PROBLEM

Creation of an isothermal map for the State of Washington is important because current AASHTO specifications [1] used in highway design practices include only two temperature ranges, one for "moderate climate" conditions and one for "cold climate" conditions. These ranges are defined for different structural types as follows:

	Range
Metal Structures:	
Moderate climate, from 0 to 120°F	66.7°C (120°F)
Cold climate, from -30 to 120°F	83.3°C (150°F)
Concrete Structures:	
Moderate climate, rise 30°F and fall 40°F	38.9°C (70°F)
Cold climate, rise 35°F and fall 45°F	41.1°C (80°F)

The rise or fall in temperature for concrete structures is added to or subtracted from the assumed temperature at the time of construction. The uniform longitudinal expansion of a bridge specified by AASHTO is calculated with the following equation [1]:

$$\Delta_T = \alpha L \Delta T \quad (1)$$

where α = coefficient of thermal expansion in m/m/°C

L = expansion length of bridge in m

ΔT = recommended bridge temperature range in °C

The AASHTO specification does not define which areas are considered "cold climate" or "moderate climate." An examination of extreme bridge temperature maps for Washington State shows that more than half of the bridge temperature values are outside the design temperature ranges recommended by AASHTO [66.7°C to 83.3°C (120 to 150°F)] for metal or composite bridges. For these areas the bridge movements could be

either over-or under-estimated. Therefore, a map that shows the different bridge temperature ranges across Washington State is essential for economical bridge design.

The effects of thermally induced stresses and their corresponding movements are a major concern in bridge design. It is important that these movements be accurately predicted. If the movements are over-estimated, the structure will require excessive movement capacity in the bearings and expansion joints. This capacity will increase the cost of bridge construction. If the movements are under-estimated, large internal forces may develop within the bridge structure that may lead to large-scale cracking and spalling in the abutments and superstructure. This will result in increased repair costs or a reduction in the service life. Figure 1 shows the various parts of a typical bridge.

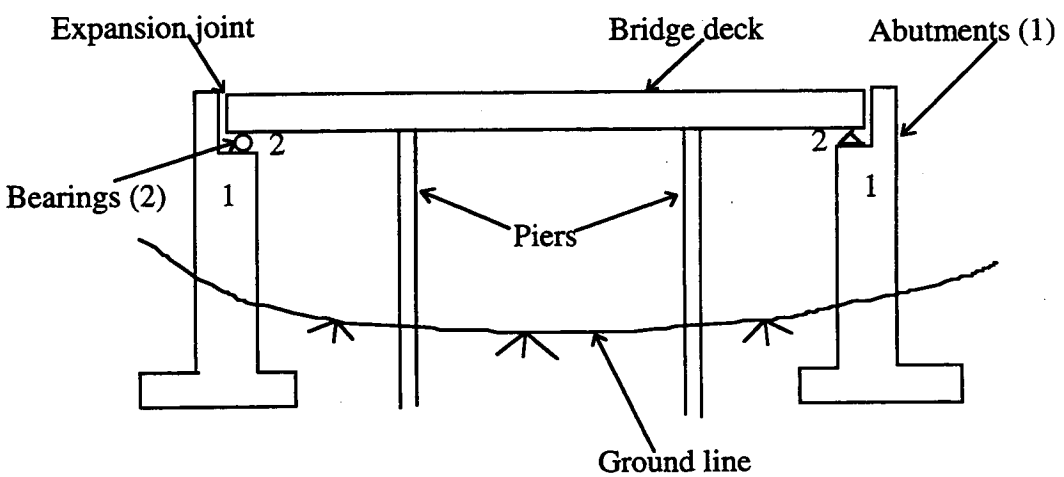

Figure 1. Different components of a bridge structure

The equation from the 1994 AASHTO specification for the calculation of wind pressure on structural supports for highway signs, signals and luminaires is given below as:

$$P = 0.0473*(1.3V)^2 C_d C_h \qquad [P = 0.00256*(1.3V)^2 C_d C_h] \qquad (2)$$

where

P = wind pressure in Pa [psf]

V = fastest-mile wind speed in kmph [mph]

C_h = coefficient for height above ground

C_d = coefficient for drag

For this project, equation (2) was adjusted by substituting a 3-second gust wind for the fastest-mile wind speed. The primary reasons for using a 3-second gust wind speed were that (1) the ASCE 7-95 proposed standard has replaced the fastest-mile speed with the 3-second gust wind speed; (2) the U. S. National Weather Service no longer collects the fastest-mile wind speed data; and (3) 3-second gust speed data are collected at a large number of stations across the United States.

Wind loads on structures depend on many factors, including the wind speed (V), the averaging time of the wind speed (t), the velocity profile factor (C_h), the gust effect factor (G), the pressure coefficient (C_p), and other factors. The velocity profile and the gust effect factors are dependent on the averaging time of the wind speed. Therefore, when the velocity is changed from the fastest-mile speed to a 3-second gust speed, these two parameters must be adjusted. Modifications to the C_h values were obtained by comparing the velocity profiles for the fastest-mile and the 3-second gust wind speeds.

RESEARCH OBJECTIVES

The first objective of this research was to analyze the temperature data collected at 49 stations across Washington State and calculate the corresponding composite bridge temperature values. Isothermal maps were then created using a computer mapping

software program called MapInfo [3]. The temperature data were collected from the Climate Data base published by the National Climate Data Center at the University of Washington. The researchers used Moorty's [2] procedure to convert the air temperatures obtained at each station to the corresponding bridge temperatures (Moorty's use of 2-D heat transfer analysis is briefly discussed in Appendix A). The resulting isothermal map is expected to provide better information about the temperature ranges to which bridges in Washington State are subjected.

The second objective of this research was to identify the wind microclimate for Washington State. Extreme value analysis was performed to calculate the velocities corresponding to 10-year and 25-year return periods. Furthermore, the current AASHTO specification [4] for calculating pressure on structural supports was re-evaluated in light of the proposed velocity changes. This was accomplished by analyzing wind velocity data for seven stations in Washington State and by comparing the velocity profiles for the hourly, fastest-mile, and 3-second wind speeds. The proposed wind load provisions of ASCE 7-95 [5] were used in the present analysis to incorporate the changes necessitated by using a 3-second gust wind speed. Wind directionality and rose plots for the same seven locations were generated.

FINDINGS: TEMPERATURE

THERMAL BEHAVIOR OF BRIDGES

Bridge structures are subjected to complex thermal stresses, which vary continuously with time. The magnitude of these stresses is a function of the temperature variations within the bridge structure. The factors of geographic location, climatological conditions, cross-section geometry, thermal properties of the materials, and the area of the exposed surfaces influence the temperature variation [6]. Although many bridge designers recognize that temperature variations can produce high stresses, the bridge design codes provide little guidance on calculating these stresses.

The climatological factors of ambient air temperature, solar radiation, and air velocity are the most significant parameters that affect the bridge temperature [7]. In a composite steel and concrete bridge, the concrete deck is heated by solar radiation from the top surface down through the slab, while the steel beneath the deck is shaded most of the day and maintains a temperature approximately equal to the ambient temperature [6]. Thus, the temperatures on the bridge structure are not uniform across the cross-section; consequently, thermal stresses, strains, or both result. A combination of both strain and stress is usually present because the materials are never completely free to move, nor are they completely restrained. Non-uniform temperature across the cross-section of a simply supported bridge causes longitudinal stresses and, thus, longitudinal movements, whereas bridges with skews or complex geometry may experience transverse or torsional movements along with the longitudinal movements. Daily changes in temperatures (temperature differences between day and night) give rise to temperature fluctuations and variations within a bridge structure. Yearly changes in temperatures (temperature differences between summer and winter) are responsible mainly for expansive and contractive bridge deck movements relative to the time of construction [7].

The top of the bridge deck slab is usually warmer than the bottom of the bridge when the sun shines on the exposed deck. The top also cools faster than the girders when a rain or snow storm first begins. A uniform temperature may exist just before sunrise, when the air temperature has remained nearly constant for several hours. Thus a variety of temperature distributions are possible throughout the depth of a bridge [11].

Effective expansion devices are important for bridge structural integrity. Expansion devices that do not behave as expected are not only uneconomical but also can damage a bridge structure. Through knowledge of the magnitudes of thermal movements and stresses would permit a designer to make a more rational selection from among the types of bearings, expansion devices, and joint sealants.

HEAT TRANSFER PROCESS IN A BRIDGE STRUCTURE

Bridge structure surfaces, which are exposed to the atmosphere, exchange heat energy with their surroundings. Thus, a bridge structure is typically in an unsteady thermal state. The three main processes of heat transfer in a bridge structure are (1) radiation, (2) convection, and (3) conduction. An exposed concrete bridge deck continually loses and gains heat from radiation to or from the sky or surrounding objects, from convection by moving air to or from the surrounding atmosphere, and from conduction to and from the surroundings through the piers and supports. In summer during the daytime, because the heat gain is greater than the heat loss, the temperature increases throughout the structure's depth. During a typical winter night, the converse is true, and the temperature in the superstructure decreases. Heat input typical of a summer day results in positive temperature gradients in the deck; that is, the top surface is warmer than the bottom. Negative gradients, in which the top surface is cooler than the bottom, result from a net heat loss during winter nights. The heat flow processes for typical summer and winter conditions are shown in Figure 2 [8].

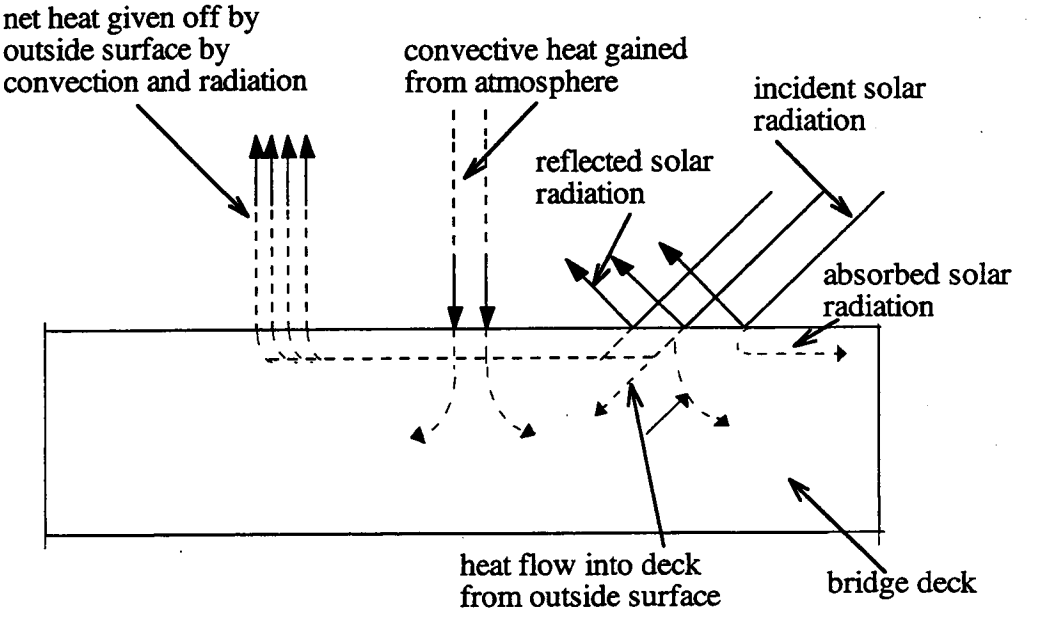

(a)

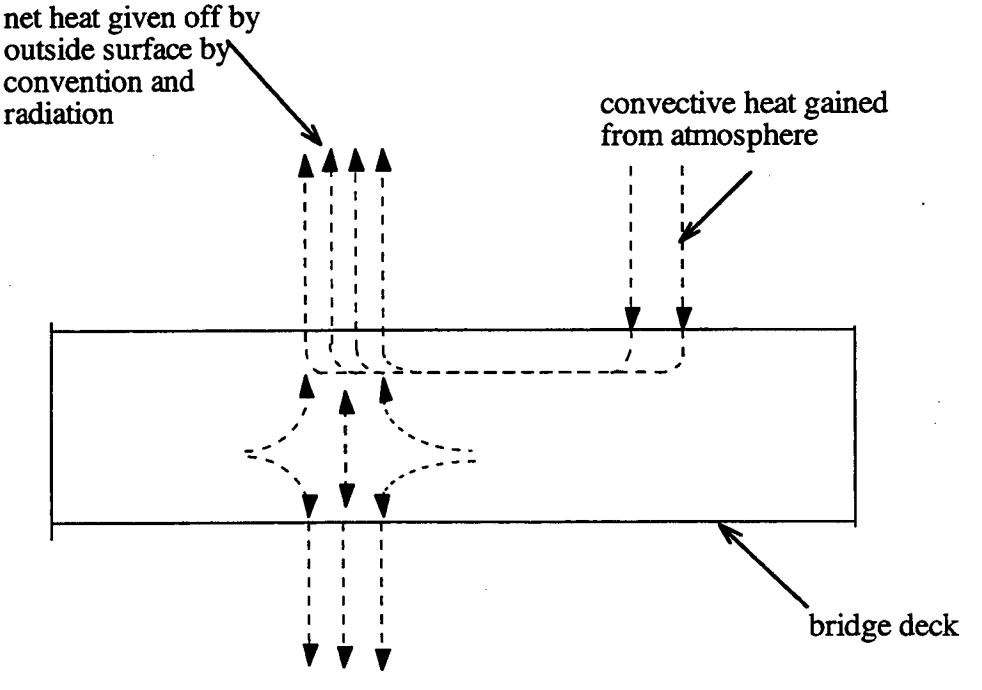

(b)

Figure 2. Heat gain and loss processes for (a) summer and (b) winter [8]

The solar radiation that is incident on the structure's surface is known as insolation and is dependent on several atmospheric conditions such as cloud cover and pollution. Solar radiation also varies with time of year. The heat transfer process that occurs in an exposed bridge structure is illustrated in Figure 3 [2]. A major portion of the solar radiation from the sun is absorbed by the atmosphere and is scattered by it. Only a small portion is incident on the bridge structure. A portion of this incident radiation is reflected back to the atmosphere from the bridge deck as shown in Figure 3. Re-radiation is the transfer of heat from the deck to the atmosphere and it usually occurs during the night. The scattered radiation from the atmosphere that is incident on the structure is known as "diffuse radiation." The bridge surface also receives radiation that is reflected from the ground. Convection by wind reduces the heat of the structural surfaces. In a high wind area, a bridge structure may lose a lot of heat through wind convection.

The general three-dimensional heat flow equation [2] that models the heat flow in a bridge structure is given below:

$$\rho c \frac{\partial T}{\partial t} = k\left(\frac{\partial^2 T}{\partial x^2} + \frac{\partial^2 T}{\partial y^2} + \frac{\partial^2 T}{\partial z^2}\right) \tag{3}$$

where

ρ = density of the medium, kg/m^3 or lb/ft^3

c = coefficient of specific heat of the medium, J/kg °C or Btu/lb. °F

k = conductivity, W/m °C or Btu/h ft °F

T = temperature of the material, °C or °F

t = time

x, y, z = coordinates of depth, width and length

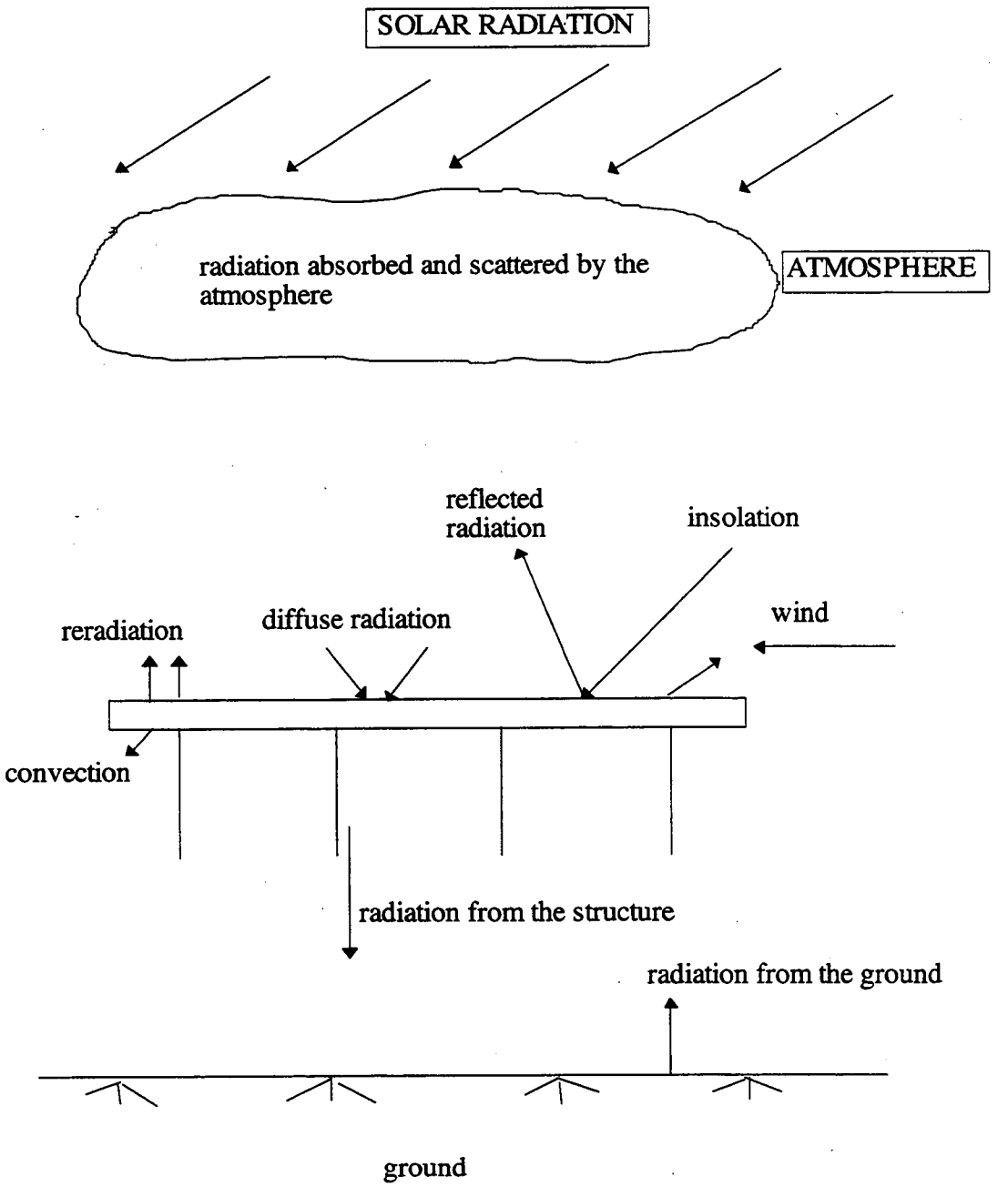

Figure 3. Heat transfer process in a bridge [2]

Maximum temperature gradients occur through the depth of the bridge. The temperatures along the width and the length are relatively uniform. For a bridge deck subjected to solar radiation, the thermal variation along the length (z - direction) of the bridge can be assumed to be constant. This simplification results in a two-dimensional heat flow equation, as follows:

$$\rho\, c \frac{\partial T}{\partial t} = k\left(\frac{\partial^2 T}{\partial x^2} + \frac{\partial^2 T}{\partial y^2}\right) \tag{4}$$

The boundary conditions [2] that satisfy the conditions of insolation, convection, and radiation can be combined together and written as follows:

$$\eta\, I_n - h_c\left(T_s - T_a\right) - \varepsilon\zeta\left(K_s^{\,4} - K_a^{\,4}\right) + k_n \frac{\partial T}{\partial n} = 0 \tag{5}$$

where

η = coefficient of absorptivity

I_n = insolation at the boundary, W/m^2 or $Btu/h\ ft^2$

T_s = temperature at the surface, °C or °F

T_a = ambient air temperature, °C or °F

K_s = absolute temperature at surface, °K or °R

K_a = absolute ambient air temperature, °K or °R

k_n = conductivity of the material in the direction normal to the surface, W/m °C or Btu/h ft °F

h_c = coefficient of convective heat transfer, W/m^2 °C or $Btu/h\ ft^2$ °F

ζ = Stefan-Boltzman constant = $5.67*10^{-8}\ W/m^2\ K^4$ or $Btu/h\ ft^2\ R^4$

ε = the emissivity coefficient that relates the radiation of a gray surface to that of an ideal black body

The radiation heat transfer [2] can be expressed as follows:

$$\varepsilon \varsigma \left(K_s^4 - K_a^4\right) = \varepsilon \varsigma \left(K_s + K_a\right)\left(K_s^2 + K_a^2\right)\left(T_s - T_a\right) \quad (6)$$

$$= h_r \left(T_s - T_a\right) \quad (7)$$

where h_r is the radiative heat transfer coefficient and is equal to $\varepsilon\varsigma(K_s + K_a)(K_s^2 + K_a^2)$. On combining $h_c + h_r = h$, where h is the total heat transfer coefficient, the boundary conditions become [2]

$$\eta I_n - h(T_s - T_a) + k_n \frac{\partial T}{\partial n} = 0 \quad (8)$$

The procedure adopted by Moorty [2] for the heat transfer analysis and the development of the mean bridge temperature equations are presented in Appendix A.

MEAN BRIDGE TEMPERATURE VALUES FOR WASHINGTON STATE

Equations obtained from Moorty's analysis were used to obtain the maximum, minimum, and range of mean bridge temperatures for composite bridges from the maximum, minimum, and range of ambient air temperatures.

Procedure

For the purpose of this research, the temperature records for 49 stations were obtained from the Climate Data Base published by the National Climate Data Center (NCDC). Temperature records were obtained for stations that have records for at least 43 years. Stations at Walla Walla (20 years of data) and Quillayute (25 years of data) were included, even though the number of records is less than 43 years because the statistics for these data were not significantly different from the neighboring stations.

The air temperature range was calculated by subtracting the minimum temperature from the maximum temperature. The maximum and minimum air temperatures that were used for this project were the extreme values. The researchers obtained these values by first determining the maximum recorded temperature for each month of every year and then selecting the maximum among those values for all the years

considered. Similarly, the minimum air temperature at any station is the minimum of all the minimum air temperatures ever recorded at that station. For this project, the maximum, minimum, and range of air temperatures were then converted to the corresponding mean bridge temperatures using equations A-6, A-7, and A-8 (Appendix A). The results obtained are shown in Table B-1 of Appendix B. The bridge temperature values obtained using the above equations are conservative values because Moorty's equations were based on average temperature instead of extreme maximum or minimum values.

The computer mapping program MapInfo was used to plot the temperature values for Washington State. Several maps of Washington State were created to show the temperature patterns of the state based on the maximum, minimum and range of air temperature values. Maps that show the regions outside the AASHTO ranges and the different bridge temperature ranges were also created. The isothermal map of Washington State for composite bridges was developed based on the mean bridge temperature ranges at different stations. All these maps are shown on the following pages.

Explanation of the Maps

Figures 4 and 5 are maps based on the extreme maximum and minimum temperatures. These two maps describe the temperature patterns across Washington State in summer and in winter. An examination of these maps shows that the eastern half of the state is subjected to higher temperature variations than the western half. For the eastern part, the maximum temperature in summer lies between 41 to 47°C (106 to 115°F), and the minimum temperature in winter is between -29 to -44°C (-21 to -50°F). The western half experiences temperatures between 31 to 40°C (86 to 105°F) during summer and -14 to -28°C (7 to -19°F) during winter. The western part, which includes the coastal region, has a cooler summer and warmer winter than the eastern. Figure 6, based on the maximum range of air temperature, illustrates this phenomenon.

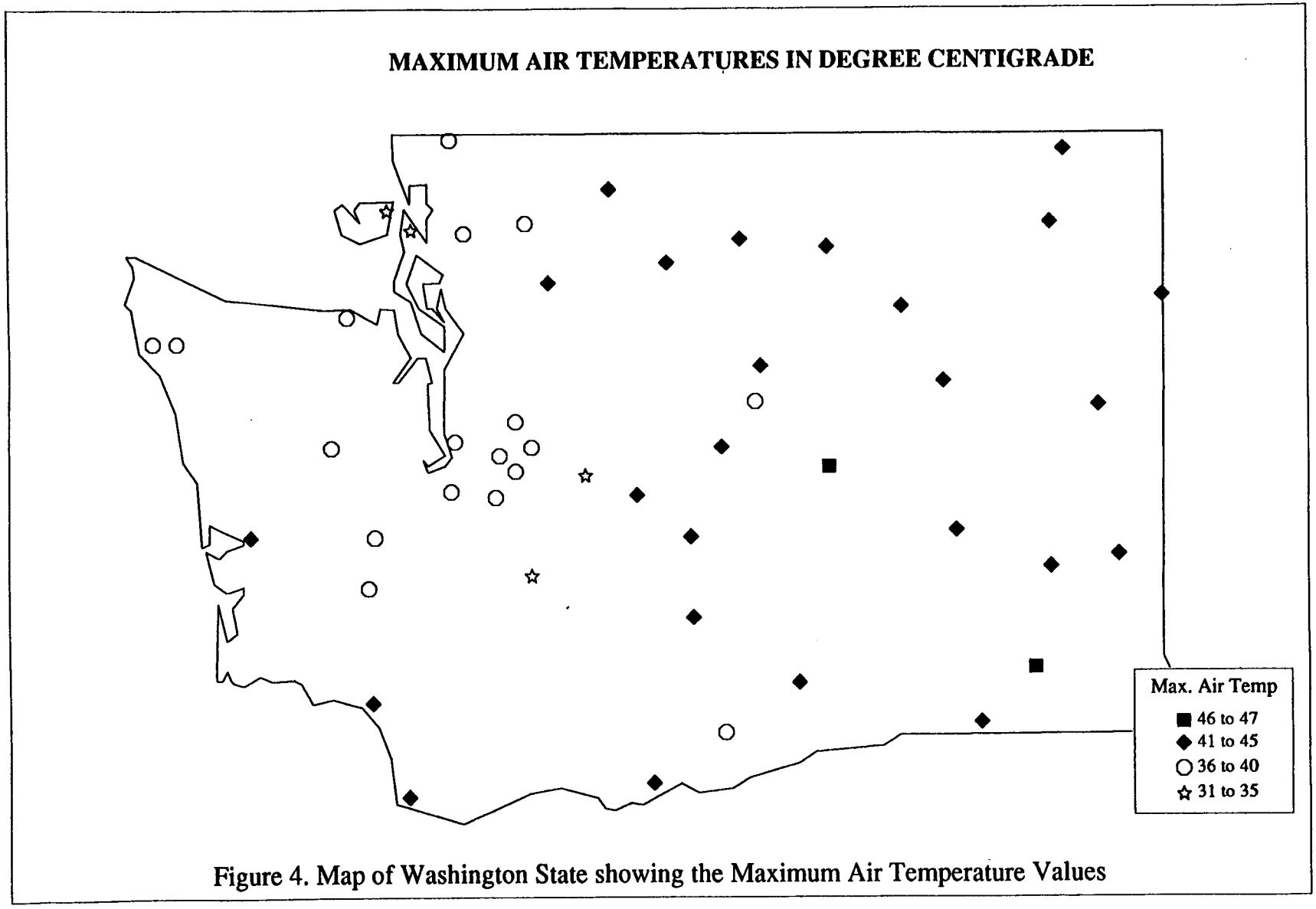

Figure 4. Map of Washington State showing the Maximum Air Temperature Values

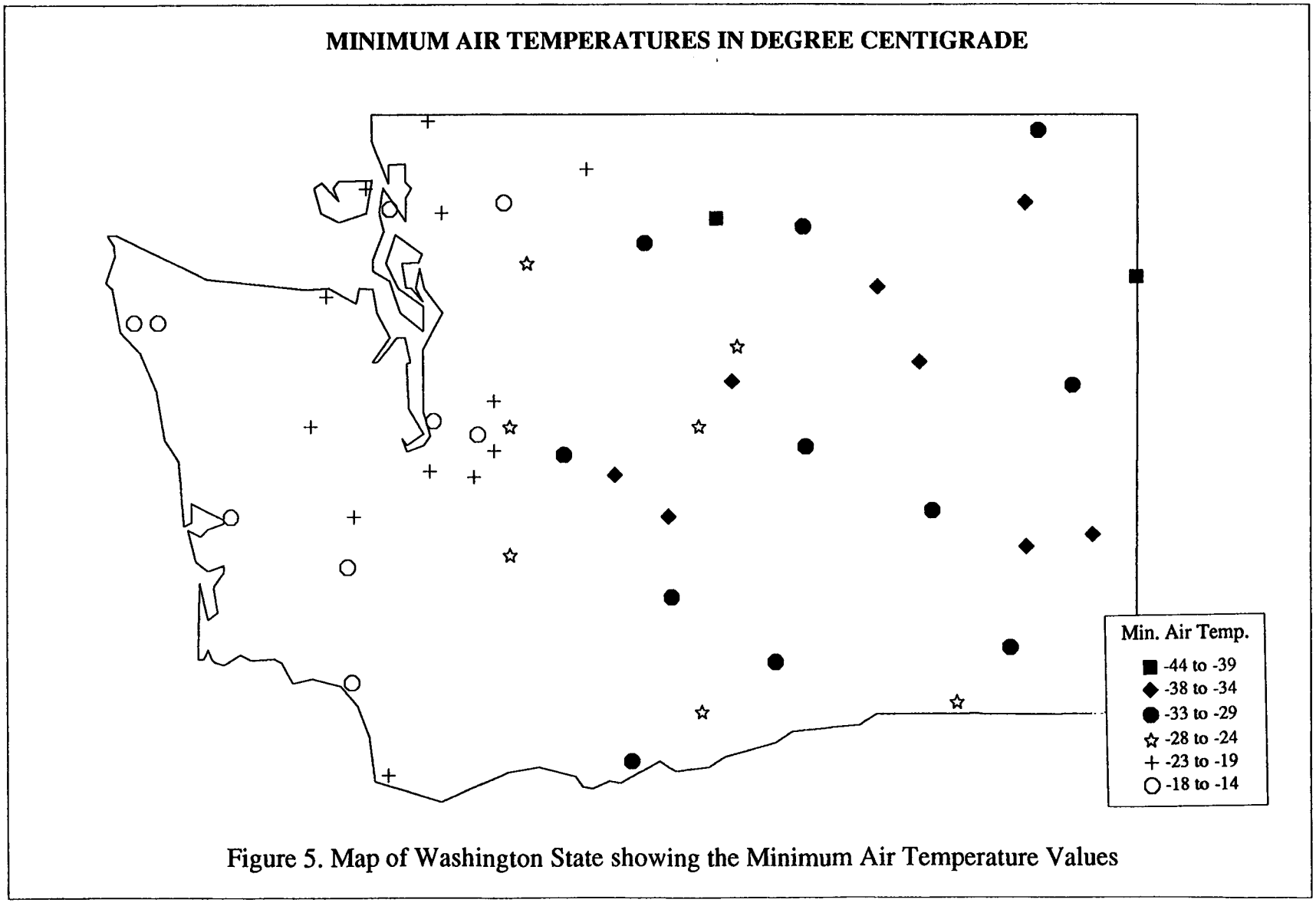

Figure 5. Map of Washington State showing the Minimum Air Temperature Values

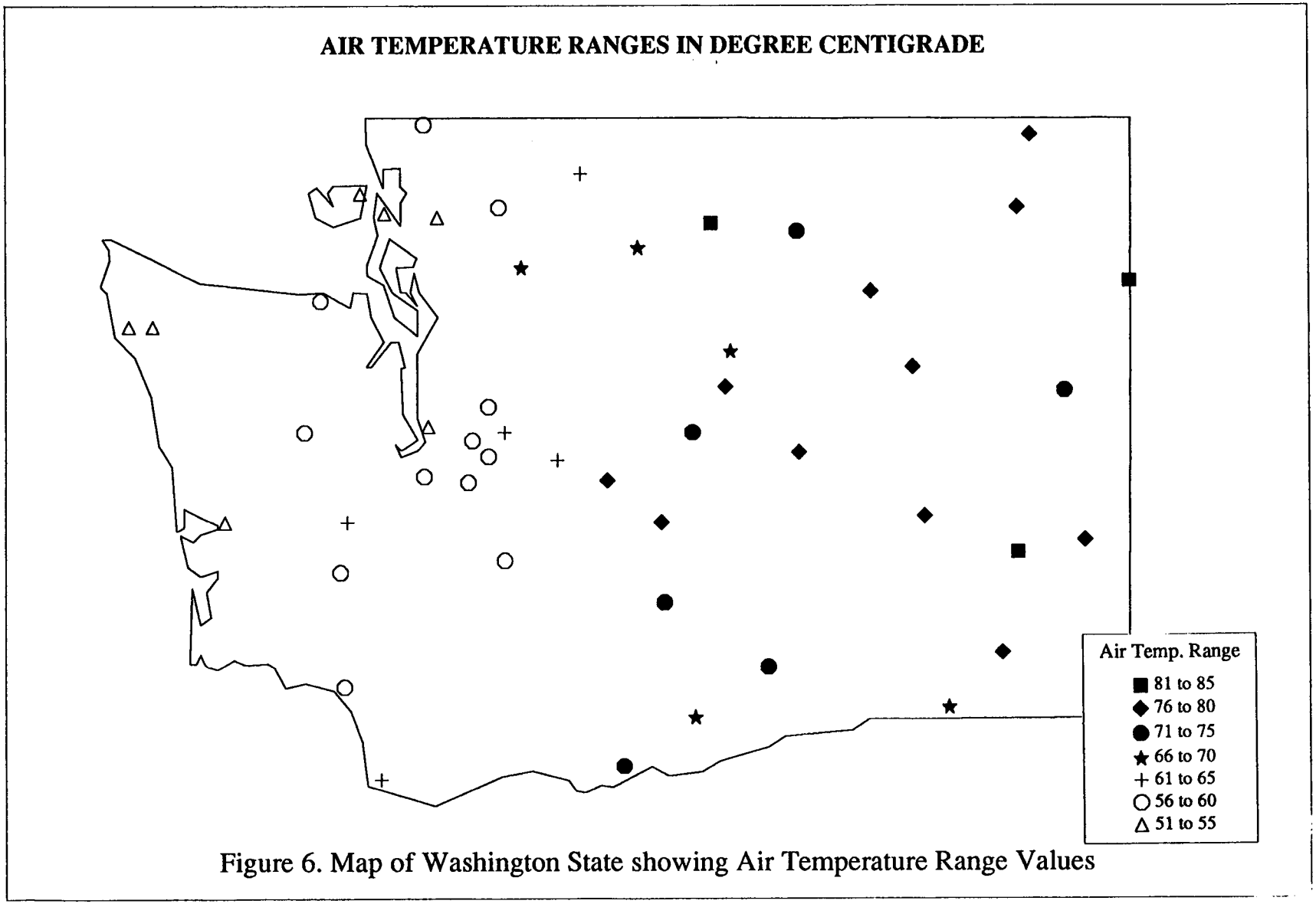

Figure 6. Map of Washington State showing Air Temperature Range Values

Figure 7 shows the regions that have temperature ranges below or above the AASHTO values. It is evident that more than half of the data points fall outside the specification ranges. Figures 8 and 9 show the expected maximum and minimum temperatures that bridges could experience during their service lives in different regions during summer and winter, respectively. However, the maximum range of temperatures that any bridge could experience is the most important factor to consider when bridges are designed for thermal movements. These bridge temperature range values are plotted in Figure 10. A contour map based on these ranges is also shown in Figure 11. An examination of the maximum, minimum, and range of bridge temperature maps reveals that the minimum bridge temperatures have the greatest effect on expected bridge temperature ranges because the minimum values vary between -9°C to -43°C (a 32°C range), whereas the maximum values vary between 36°C to 52°C (a 16°C range). The contour values increase in 5°C increments from the west part of the state at 55°C to the east at 85°C. Thus, seven ranges are covered in this map, depending on the various temperature patterns. Using this map can help designers avoid over-predicting bridge movements near the coastal region and under-predicting movements near the eastern part of Washington State.

The maps discussed above depend on the elevation of the stations considered. A study of the effect of elevation on temperature was also undertaken to find a way to compare temperature values from the same elevation.

Effect of Elevation on Temperature

The purpose of this analysis was to eliminate the effect of elevation on air temperatures measured at each station, so that temperature contour values could be based on the same elevation at all stations. All elevations referred to here are measured from the mean sea level. In the previous case, the contour values were calculated on the basis of the temperature values measured at the stations, which are located at different elevations. For example, Aberdeen is located 3 m (10 ft) above sea level, and its

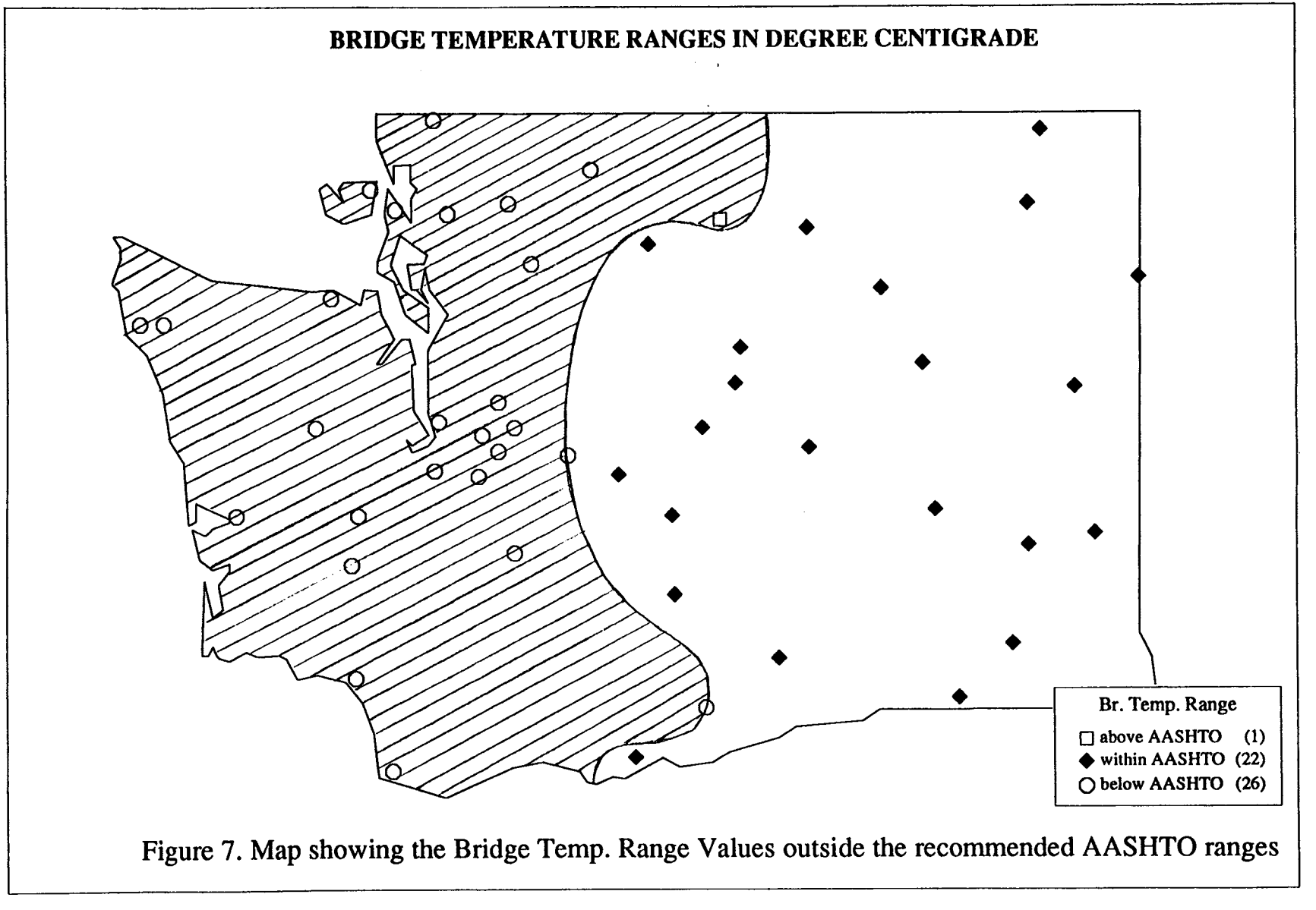

Figure 7. Map showing the Bridge Temp. Range Values outside the recommended AASHTO ranges

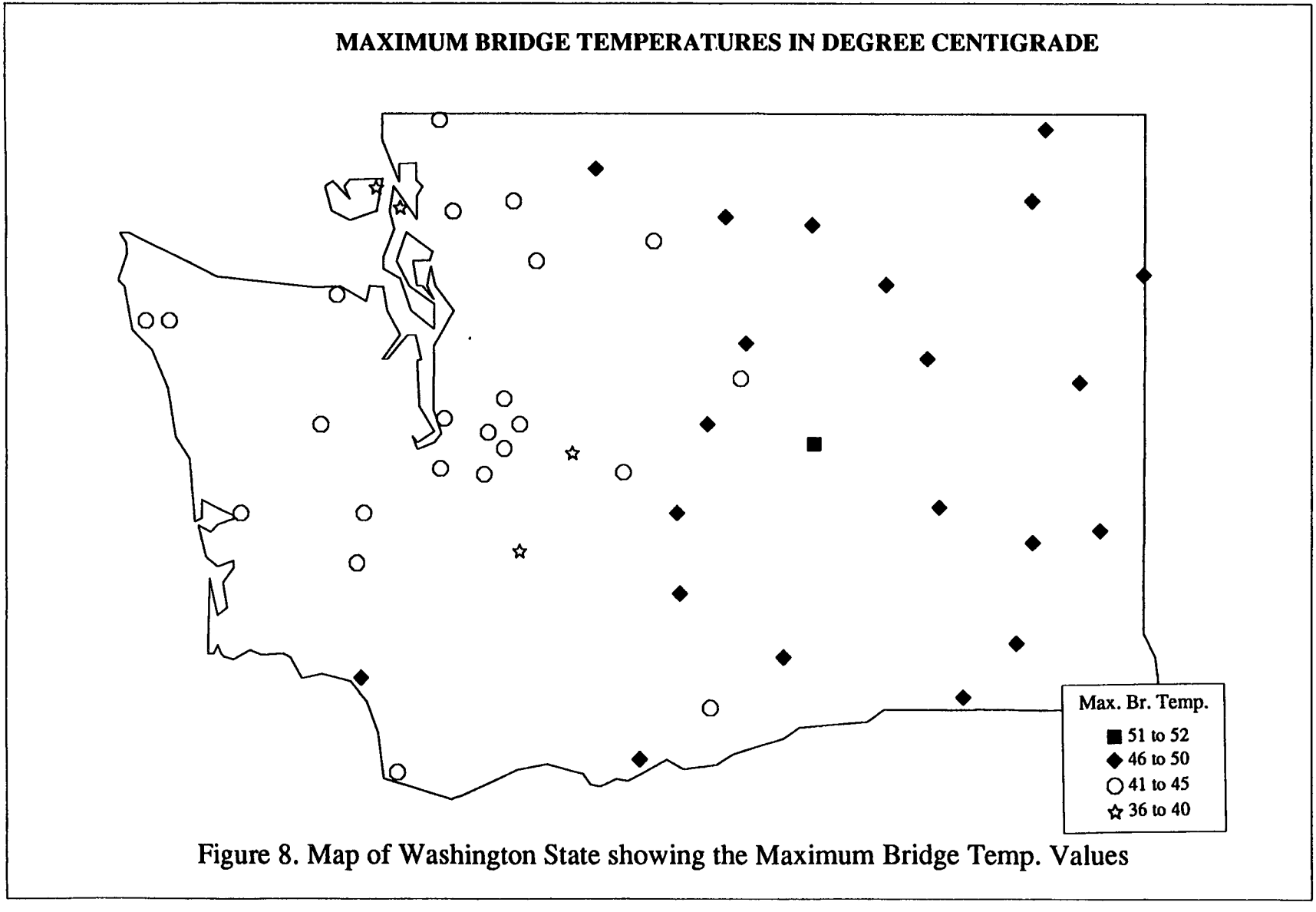

Figure 8. Map of Washington State showing the Maximum Bridge Temp. Values

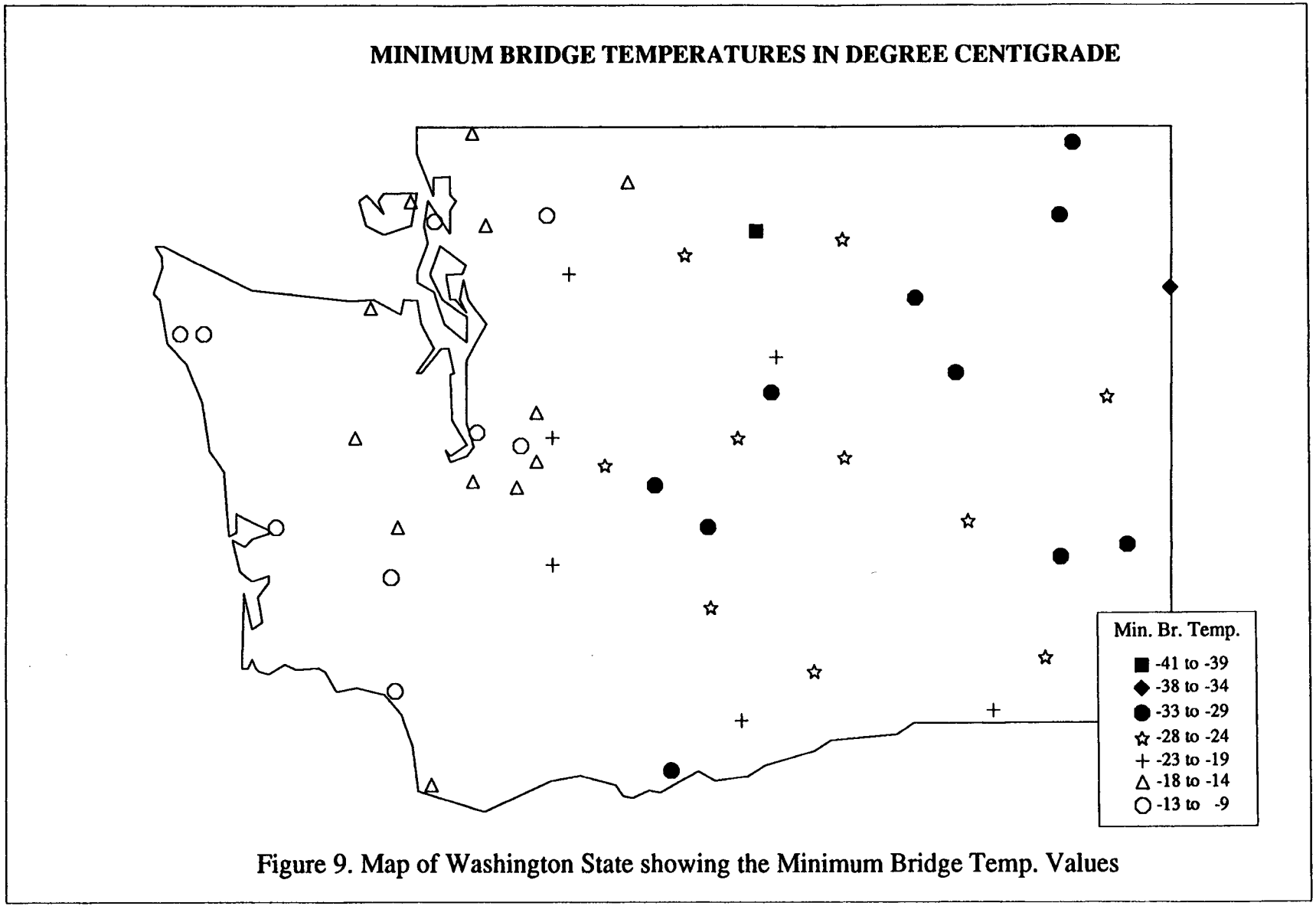

Figure 9. Map of Washington State showing the Minimum Bridge Temp. Values

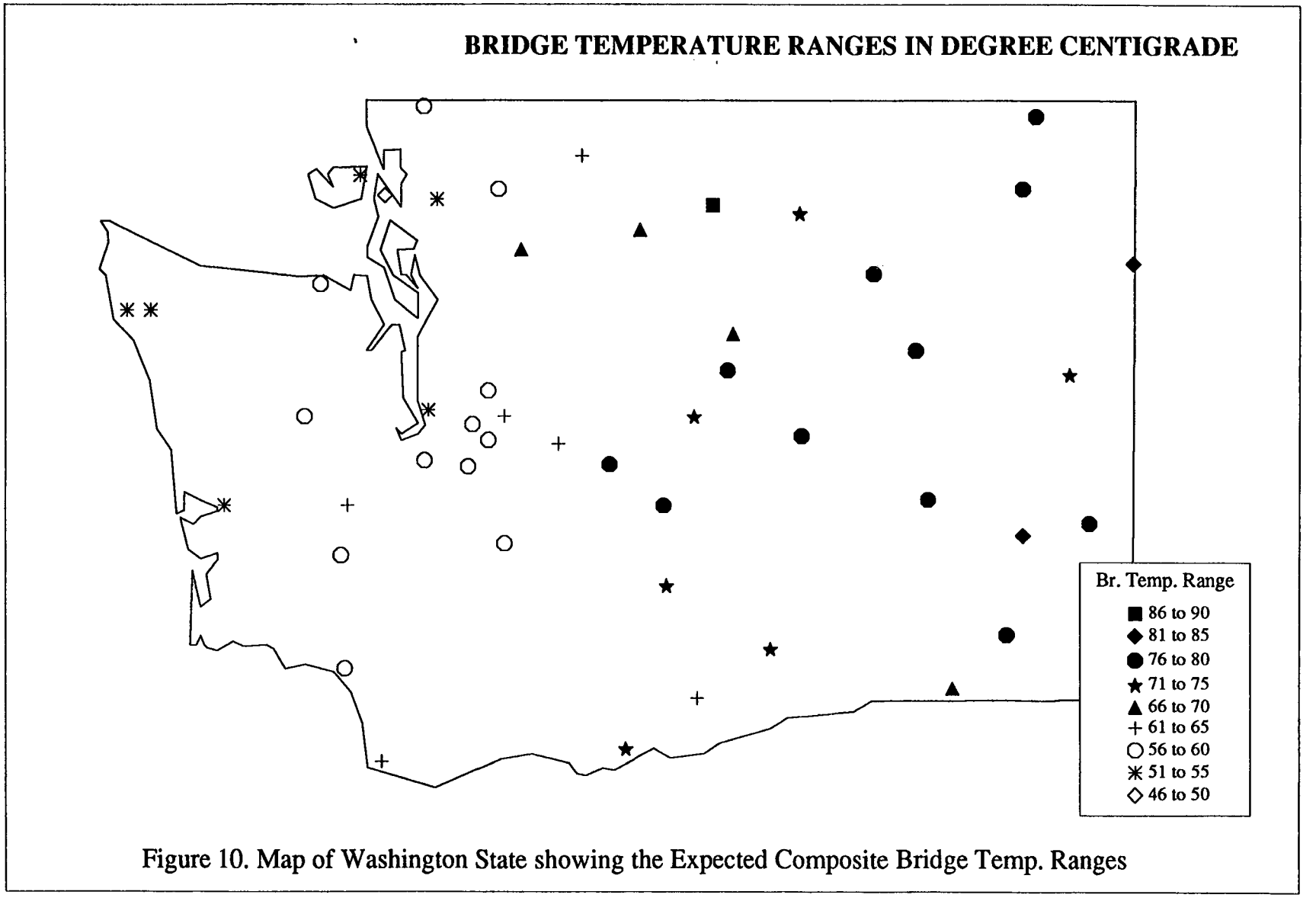

Figure 10. Map of Washington State showing the Expected Composite Bridge Temp. Ranges

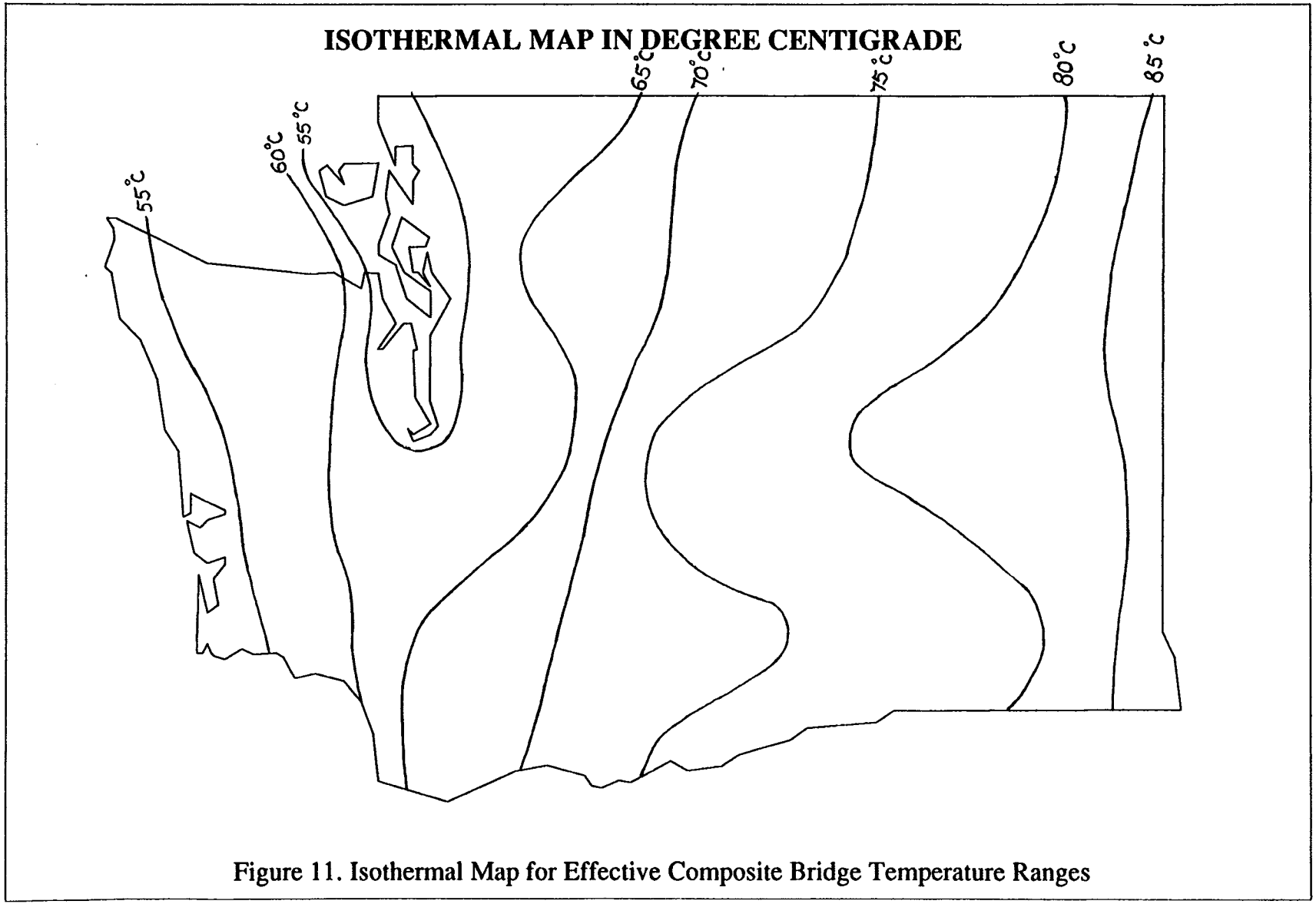

Figure 11. Isothermal Map for Effective Composite Bridge Temperature Ranges

maximum and minimum temperatures are 41°C and -14°C (105°F and 6°F), respectively. Bickleton is located 915 m (3000 ft) above sea level, and its maximum and minimum temperatures are 39°C and -27°C (102°F and -17°F), respectively. The maximum temperature values do not change considerably as the elevation changes, but the minimum temperature values vary greatly, depending on the elevation. Therefore, an analysis was necessary to eliminate the effect of elevation on air temperatures before they were converted to bridge temperature values.

For this analysis, relationships between elevation and maximum, minimum, and range of air temperatures were obtained by fitting curves between elevation and corresponding air temperatures. Figure 12 shows that the maximum air temperature increases gradually as the elevation increases. After an elevation of about 497 m, the maximum air temperature starts to decrease at about the same rate. Figure 13 shows that the minimum air temperature decreases as the elevation increases, up to about 537 m. After that, the temperature gradually increases at a slower rate. Figure 14 shows that the range of air temperature increases as the elevation increases. After about 537 m, the air temperature range starts to decrease at a slower rate. All three graphs show a marked change at about 500 m. Linear regression analyses were performed for elevations up to and beyond 500 m for all three cases.

From the regression analysis, equations relating elevation to temperature were obtained. These equations are presented below.

Maximum Air Temperature

Elevation $\leq$ 497 m, Max. Air Temp. (°C) = 0.0115*Elv. + 37.80 (9a)

Elevation > 497 m, Max. Air Temp. (°C) = -0.011*Elv. + 48.97 (9b)

Minimum Air Temperature

Elevation $\leq$ 537 m, Minimum Air Temp. (°C) = -0.0345*Elv. - 16.20 (10a)

Elevation > 537 m, Minimum Air Temp. (°C) = 0.0078*Elv. - 38.87 (10b)

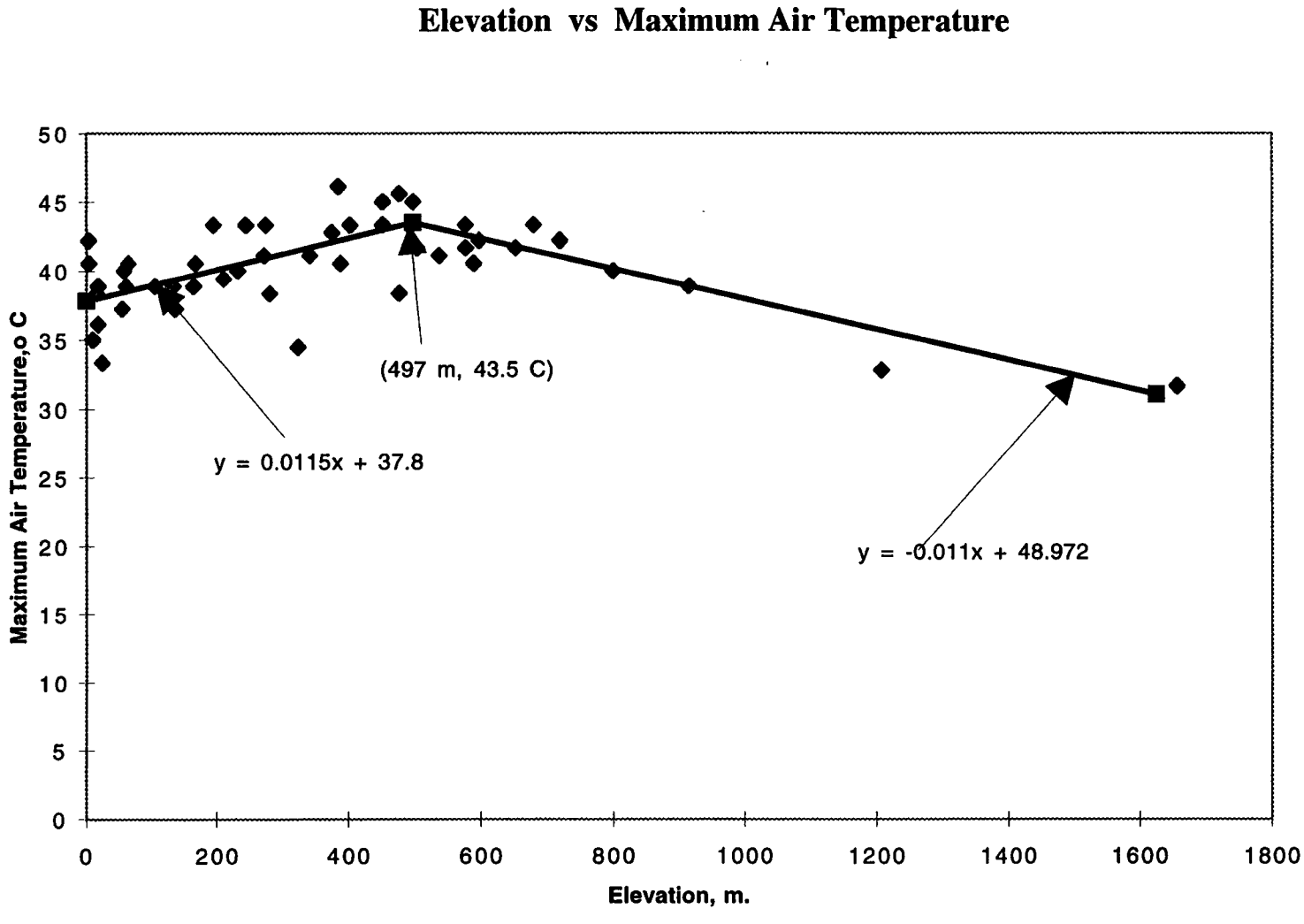

Figure 12. Relation between Elevation and Maximum Air Temperature

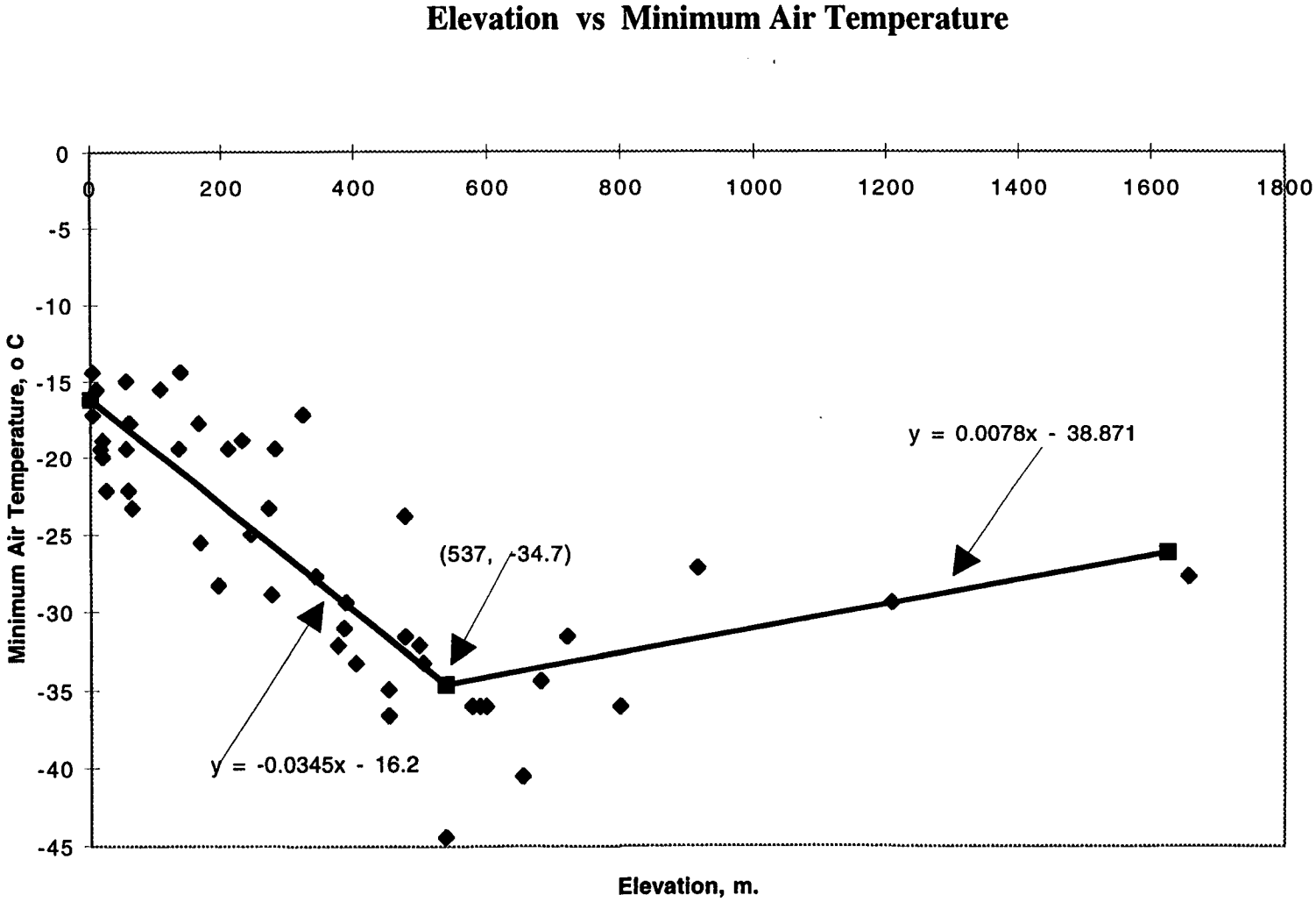

Figure 13. Relation between Elevation and Minimum Air Temperature

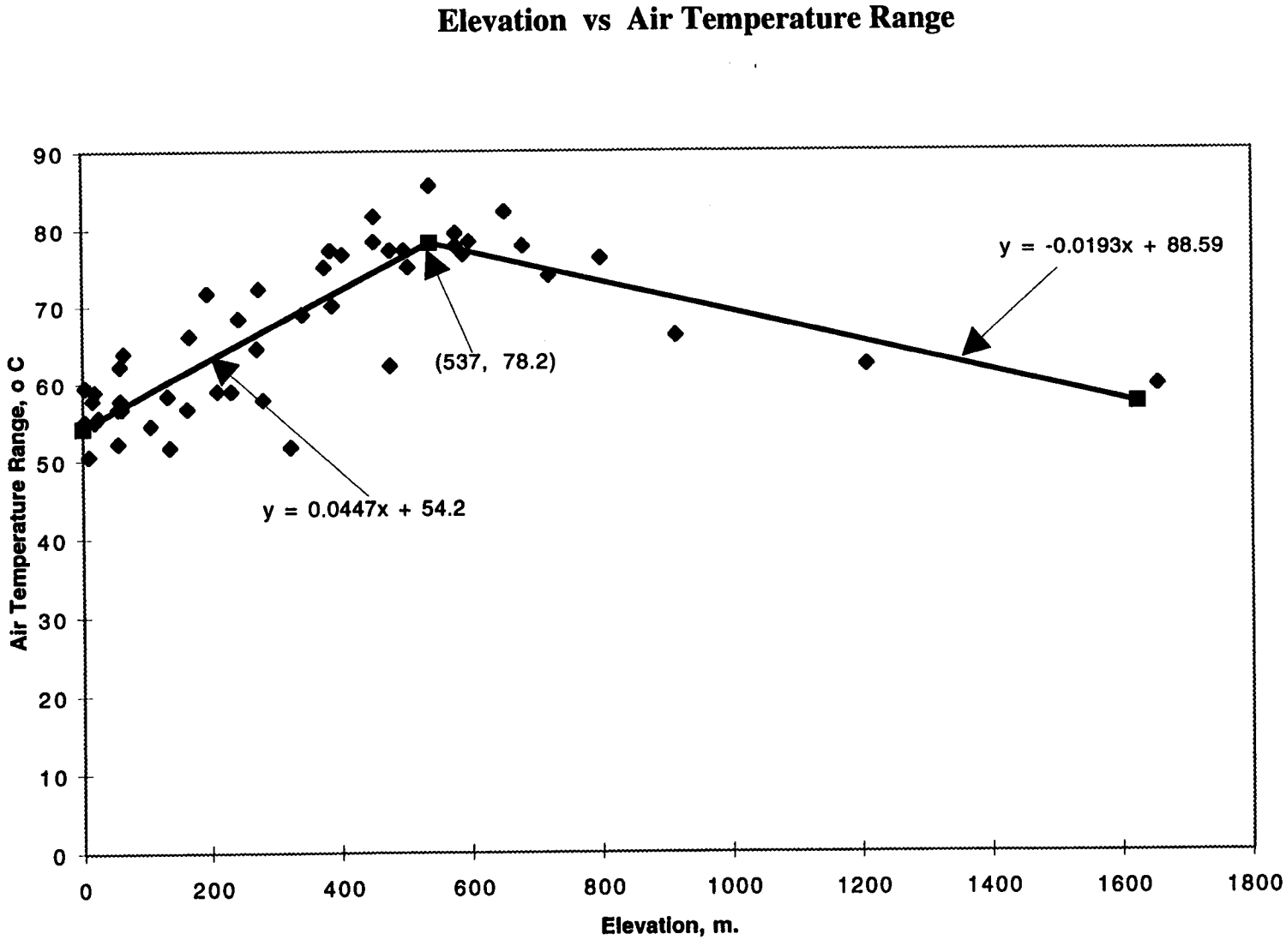

Figure 14. Relation between Elevation and Range of Air Temperature

Air Temperature Range

Elevation ≤ 537 m, Air Temp. Range (°C) = 0.0447*Elv. + 54.20 (11a)

Elevation > 537 m, Air Temp. Range (°C) = -0.0193*Elv. + 88.59 (11b)

where the factors multiplied by the elevation are the elevation factors (or the slope of each line from Figures 12, 13 and 14), and the factors added or subtracted are the temperatures at zero elevation (or the y-intercept of each equation) .

Adjustment of Air Temperature Values at Each Station to Values at Zero Elevation

To eliminate the effect of elevation, the product of the elevation and the corresponding elevation factor was added to or subtracted from the air temperature values (maximum, minimum, and range) at each station. The product of elevation and the elevation factor was added when the temperature decreased as the elevation increased, and it was subtracted when the temperature increased as the elevation increased. The adjusted equations for each case are given below.

Adjusted Maximum Air Temperature

Elevation ≤ 497 m, $(T_{max.})_{adj}$ (°C) = $(T_{max})_{meas.}$ – 0.0115*Elv. (12a)

Elevation > 497 m, $(T_{max.})_{adj}$ (°C) = $(T_{max})_{meas.}$ + 0.011*Elv. + (37.8 – 48.97)(12b)

Adjusted Minimum Air Temperature

Elevation ≤ 537 m, $(T_{min.})_{adj}$ (°C) = $(T_{min})_{meas.}$ + 0.0345*Elv. (13a)

Elevation > 537 m, $(T_{min.})_{adj}$ (°C) = $(T_{min})_{meas.}$ – 0.0078*Elv. + (-16.2 + 38.87)(13b)

Adjusted Air Temperature Range

Elevation ≤ 537 m, $(T_{range})_{adj}$ (°C)= $(T_{range})_{meas.}$ – 0.0447*Elv. (14a)

Elevation > 537 m, $(T_{range})_{adj}$ (°C)= $(T_{range})_{meas.}$+ 0.0193*Elv. + (54.2 – 88.59)(14b)

The adjusted mean bridge temperature values were calculated on the basis of the adjusted air temperature values using the following equations (equations A-6, A-7, and A-8 from Appendix A):

$$(\theta_{max.})_{adj}\ (^{\circ}C) = 1.0116 * (T_{max.})_{adj} + 4.018 \quad (15a)$$

$$(\theta_{min.})_{adj}\ (^{\circ}C) = 1.0520 * (T_{min.})_{adj} + 6.1503 \quad (15b)$$

$$(\theta_{range})_{adj}\ (^{\circ}C) = 1.0215 * (T_{range})_{adj} - 2.0225 \quad (15c)$$

where $\theta_{max.}$, $\theta_{min.}$, and θ_{range} are the mean bridge temperatures, and $T_{max.}$, $T_{min.}$, and T_{range} are the air temperatures in $^{\circ}C$, respectively.

The adjusted values of the air and bridge temperatures are shown in Table B-2 in Appendix B. A map that displays the mean bridge temperature range values adjusted to zero elevation is shown in Figure 15. If elevation had been the only factor that affected the air temperatures at a station, the temperature values obtained at zero elevation would have been the same for all stations. Because the values shown in Figure 15 are not the same, and the points are scattered across the state, it is evident that other factors such as latitude and proximity to the ocean also affect the temperatures of a region. Figure 15 can be used to obtain the bridge temperature range at a location by noting the temperature value on the map and adding to it the product of the elevation and the elevation factor. Because Figure 15 does not give a definite pattern for the temperature ranges, it may not be as convenient to use for the design purposes. The isothermal map shown in Figure 11 appears to be more useful than Figure 15.

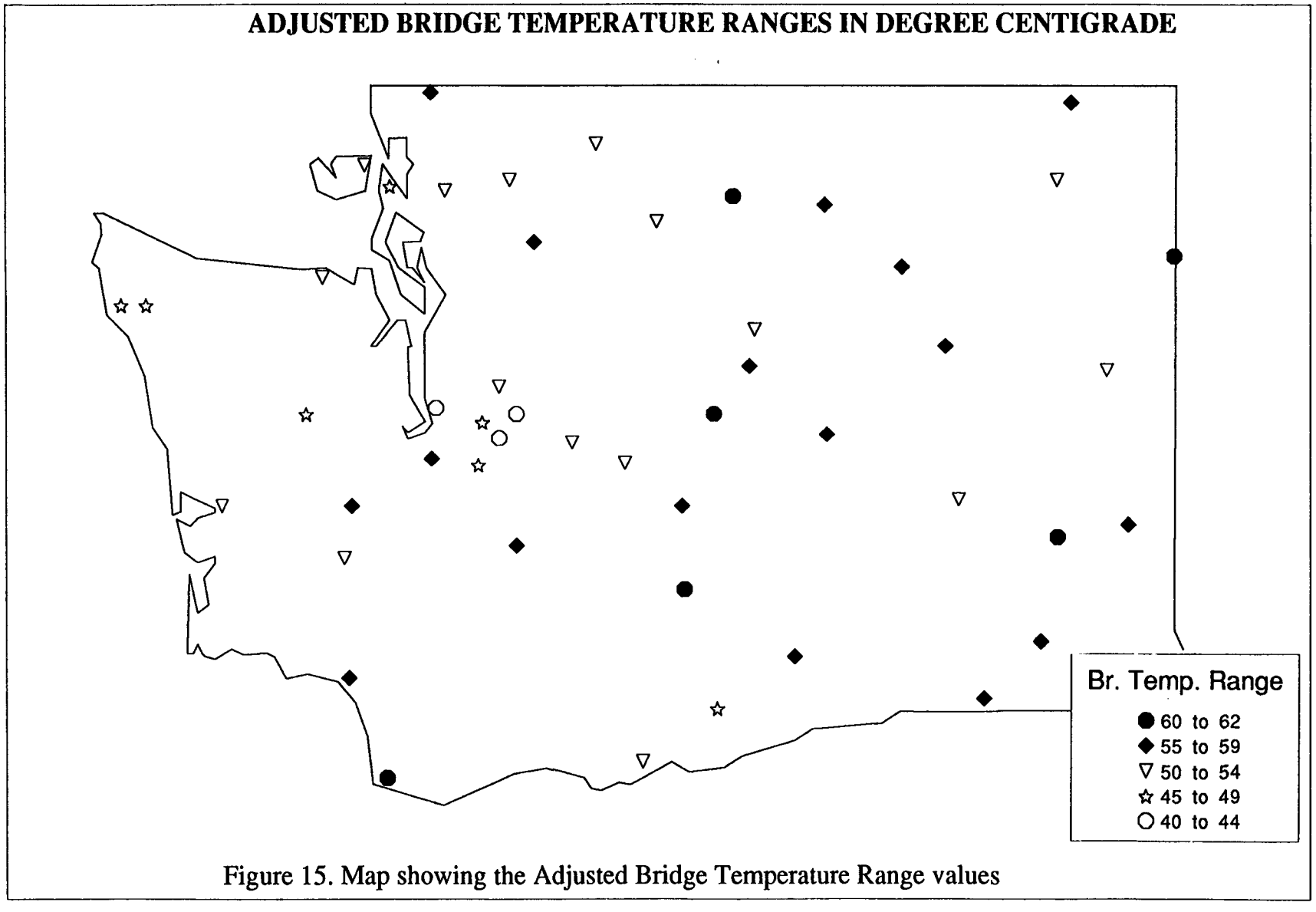

Figure 15. Map showing the Adjusted Bridge Temperature Range values

FINDINGS: WIND

BACKGROUND

The atmosphere of the earth extends about 1000 miles above the earth's surface and consists of four layers. These are, starting from the highest layer, the exosphere, the ionosphere, the stratosphere, and the troposphere. Wind occurs in the troposphere, which extends approximately 5 miles above the poles and 11 miles above the equator. Structural engineers are concerned with microscale wind flows in the atmosphere, which have a characteristic length of approximately 20 km and a duration of one hour or less. "Wind" in this context is defined as the motion of the air with respect to the earth's surface. It is primarily caused by the variable solar heating of the earth's atmosphere, as well as by differences in pressure between points of equal elevation. Such differences may be caused by the nonuniform thermodynamic and mechanical phenomena of the atmosphere.

The surface of the earth, which meets lower part of the troposphere, exerts a horizontal frictional force on the moving air, retarding the air flow. The effect of this frictional force decreases as the height above ground increases, and it becomes insignificant above a height "δ," known as the boundary layer depth or gradient height. Within the boundary layer, the mean wind speed varies from approximately zero near the ground surface to its full value, V_{gr}, at the gradient level. Beyond this level is the so-called "free atmosphere," where the wind flows with a gradient velocity. Figure 16 illustrates the boundary layer.

The gradient height depends on the terrain conditions of the earth's surface. The gradient height values are higher for comparatively rougher terrain that has large obstructions such as tall buildings or trees. For smoother terrain with fewer obstructions,

the gradient height is lower. Typical terrain conditions and corresponding gradient heights are given in Table 1 [12].

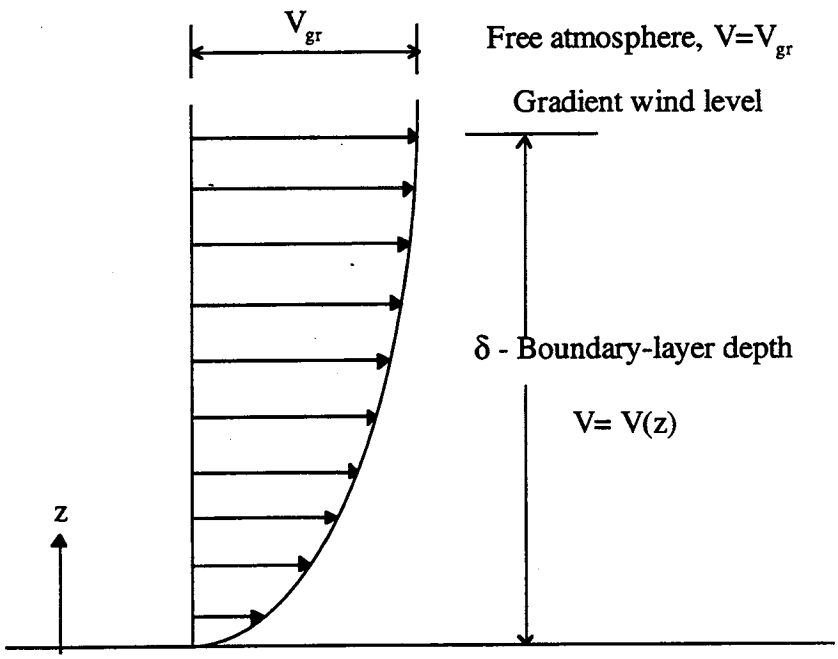

Figure 16. The atmospheric boundary layer

Table 1. Terrain and corresponding gradient heights [12]

Terrain	**Gradient height, m (ft)**
Level or slightly rolling land with some obstructions, e.g., farm land with scattered trees and buildings and airports.	290 (950)
Rolling or level country broken by numerous obstructions of various sizes, e.g., suburbs where lots are half acre or more.	351 (1150)
Broken surface with large obstructions, e.g., near suburbs with one-fourth acre or less lots and outskirts of large cities.	458 (1500)
Large obstructions, e.g., center of large city.	549 (1800)

EXTREME WIND PROBABILITY

Today structures are designed to withstand wind loads taking into account the probability of wind speed occurrence. A structure is built to provide a specific degree of safety against high winds, which is determined by the probability that winds will occur that exceed those for which the structure was designed. Exceedance probability is defined as the probability that a given wind speed will be exceeded within a one-year period. The reciprocal of exceedance probability is known as the mean recurrence interval or return period. For example, a probability of 1 percent corresponds to a mean recurrence interval of 1/0.01 or 100 years. As an illustration, consider a station in Spokane, Washington. The fastest-mile wind speed at this station based on a mean recurrence interval of 50 years is 108 kmph. This means that, on the average, Spokane is expected to experience a wind faster than 108 kmph once in a 50-year period. Thus, the probability that a wind exceeding 108 kmph will occur within a given year in Spokane is 1/50 or 2 percent.

The U.S. National standards on structural loads (ASCE 7-88) requires that ordinary structures be designed for an annual exceedance probability of 2 percent or a mean recurrence interval of 50 years. The design of crucial facilities that would pose a high risk to human life if they failed must be based on an annual exceedance probability of 1 percent or a mean recurrence interval of 100 years. The design of structures whose failure would pose a very low risk to human life can be based on an exceedance probability of 4 percent or a mean recurrence interval of 25 years.

According to AASHTO specification [4], wind load calculations for structural supports for traffic signs, signals, and luminaires consider annual probabilities of 10 percent, 4 percent, and 2 percent, or mean recurrence intervals of 10 years, 25 years, and 50 years, respectively. The annual wind exceedance probability of failure for a structure is based on its life expectancy and the risk posed to human life in case of its failure. The design of road side signs, which have a relatively short life span and pose less risk to

human life, has been based on a probability of 10 percent. The design of taller luminaire support structures has been based on a probability of 2 percent, and the design of support structures with heights of less than or equal to 15.24 m have been based on a probability of 4 percent.

The Type I Extreme Value Distribution is used to find the wind velocity associated with a particular mean recurrence interval or annual probability of occurrence for a storm. The equation [16] used to estimate the wind velocity fitted by a Type I distribution for a given probability is

$$X = \overline{X}\left\{1 + \frac{S_D(x)}{\overline{X}}[y - 0.5772]\frac{\sqrt{6}}{\pi}\right\} \tag{16}$$

where X = velocity in kmph (mph)

$\overline{X}$ = mean of X kmph (mph)

$S_D(x)$ = standard deviation of X

y = $-\ln(-\ln(1 - 1/N))$

N = mean recurrence interval

For the six stations considered in Washington State, the velocities corresponding to mean recurrence intervals of 10 and 25 years were calculated from the velocities for a 50-year period with equation 16. The results obtained are shown in Table 2. A sample calculation for the velocities at the station in Olympia is presented below to illustrate the steps.

V_{fm}^{50} = 113 kmph (69.9 mph)

N = 50 years; therefore, $y = -\ln(-\ln(1 - 1/50)) = 3.9$

$113 = \overline{X}\ \{1 + 0.12\,(3.9 - 0.5772)\,6^{0.5}/\pi\}$

where $S_D(x)\,\overline{X}$ = 0.12 is an acceptable estimate

$\overline{X}$ = 86.19 kmph

Table 2. Velocities corresponding to 50, 25, and 10 year mean recurrence intervals

Station	V_{fm}^{50} kmph(mph)		V_{fm}^{25} kmph(mph)		V_{fm}^{10} kmph(mph)	
Olympia	113.0	(69.9)	107.34	(66.39)	99.7	(61.66)
Quillayte	87.0	(53.8)	82.64	(51.12)	76.73	(47.46)
Seattle	111.2	(68.8)	105.63	(65.34)	98.12	(60.69)
Spokane	108.0	(66.8)	102.6	(63.47)	95.28	(58.93)
Walla Walla	143.2	(88.6)	136.03	(84.15)	126.37	(78.16)
Yakima	116.8	(72.25)	110.96	(68.64)	103.05	(63.74)

For a mean recurrence interval of 25 years, N = 25

$$y = -\ln(-\ln(1 - 1/25)) = 3.2$$

$$V_{fm}^{25} = 86.19^{*}\{1 + 0.12(3.2 - 0.5772)6^{0.5}/\pi\} = 107.34 \text{ kmph}$$

For a mean recurrence interval of 10 years, N = 10

$$y = -\ln(-\ln(1 - 1/10)) = 2.25$$

$$V_{fm}^{10} = 86.19^{*}\{1 + 0.12(2.25 - 0.5772)6^{0.5}/\pi\} = 99.7 \text{ kmph}$$

Wind Directionality

Wind directionality plots provide a measure of the minimum and maximum wind speed for each direction at a particular site. These plots are useful when strong directional tendencies are displayed. For the five sites for which data were available, the directionality plots are given as Figures 17(a)-(e). It can be seen that winds from the southwest quadrant are generally the strongest. The implication for design purposes is that if possible, placing a sign in the SW-NE direction should be avoided.

Wind Rose Analysis

The wind rose is a different type of directional frequency analysis of wind speeds at a particular site. It portrays the percentage frequency of the number of observations at

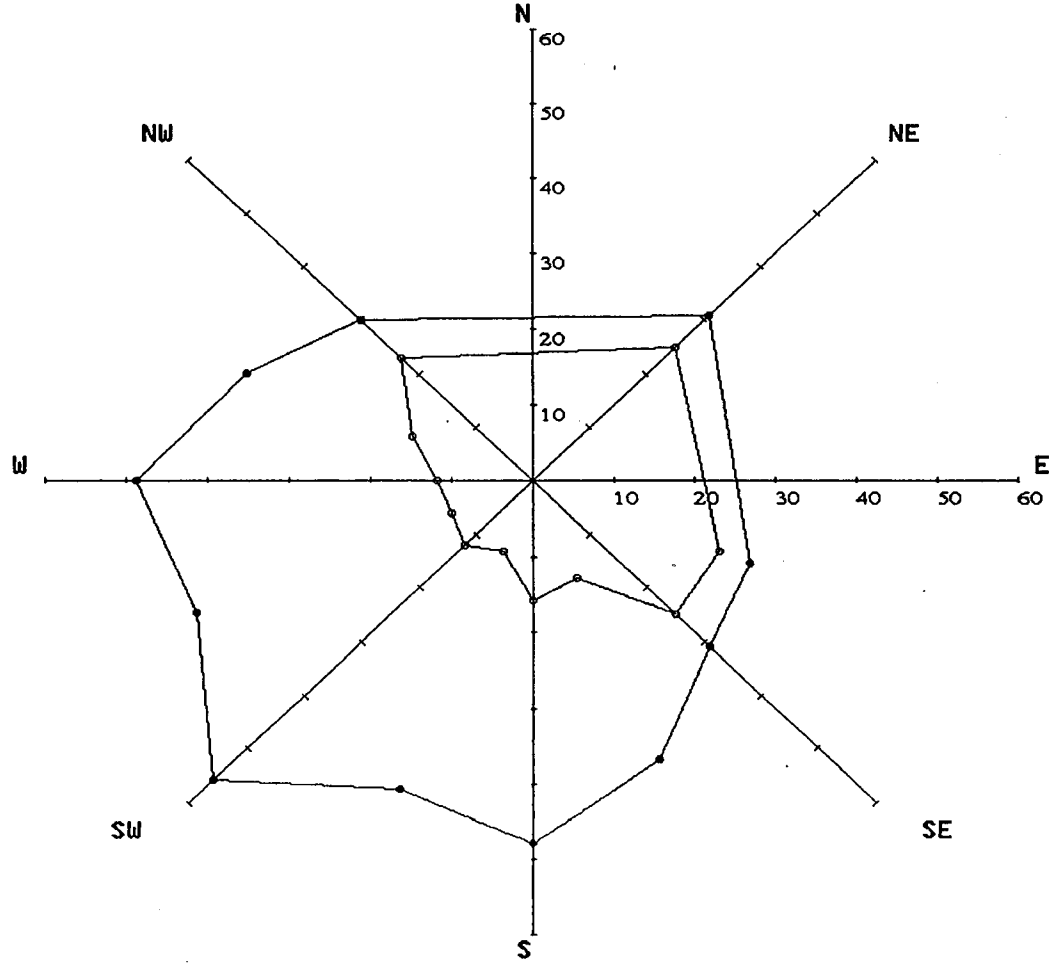

FIGURE 17(a). Wind directionality plot for Olympia using data from 1949-1992. [one knot is 1.92 m/s.]

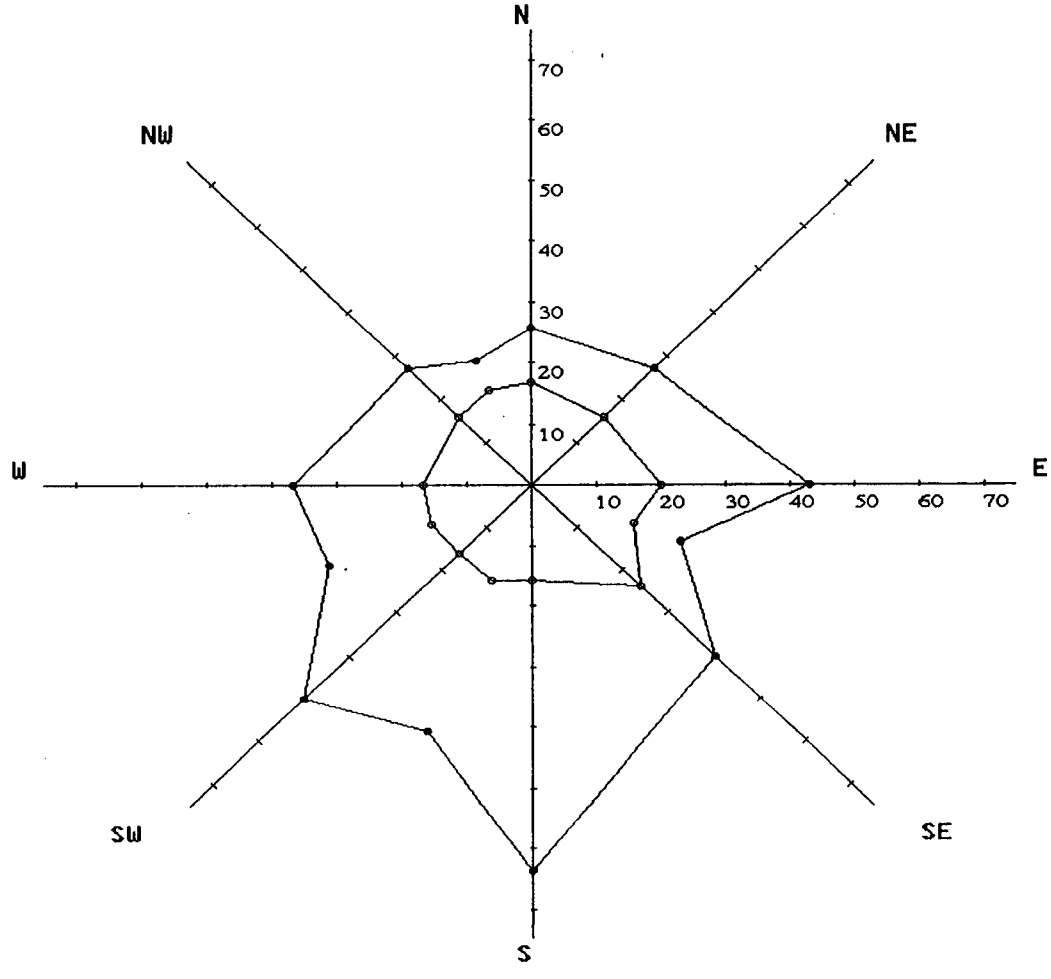

FIGURE 17(b). Wind directionality plot for Seattle using data from 1949-1992. [one knot is 1.92 m/s.]

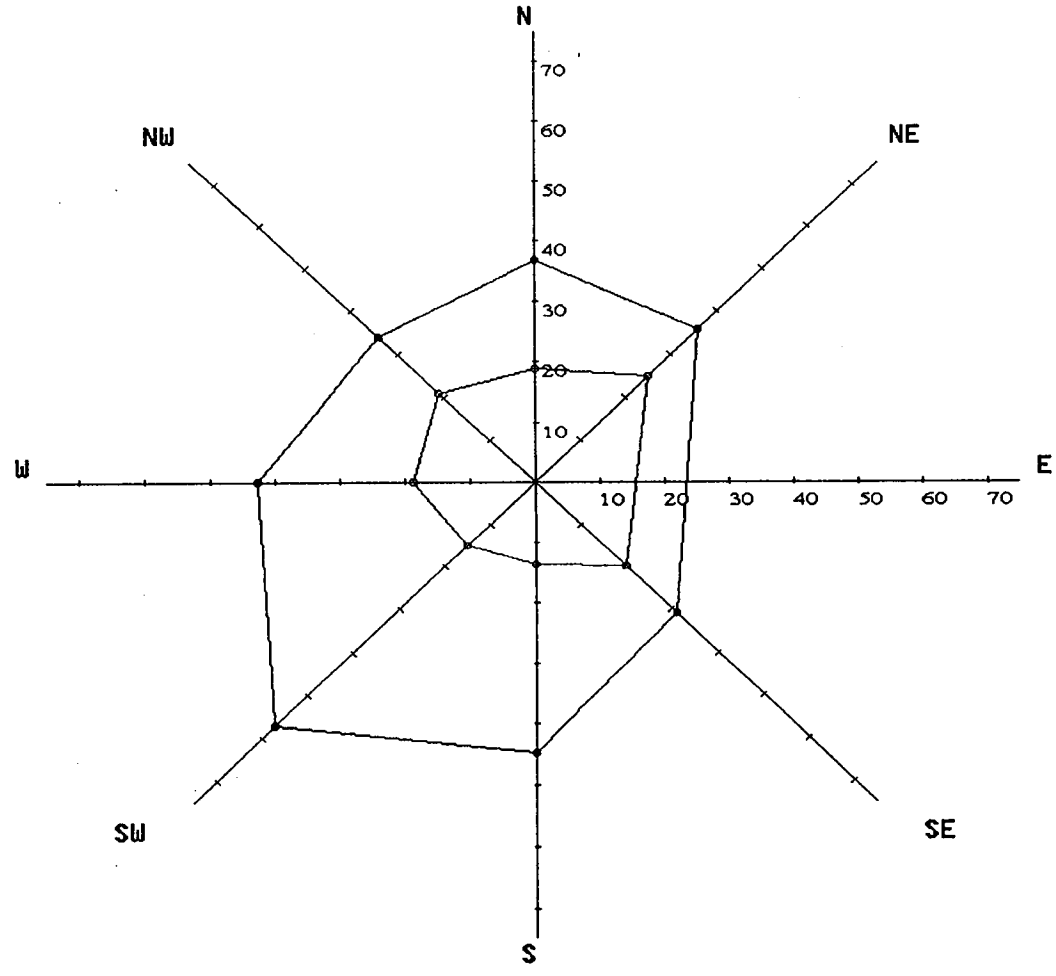

FIGURE 17(c). Wind directionality plot for Spokane using data from 1949-1992. [one knot is 1.92 m/s.]

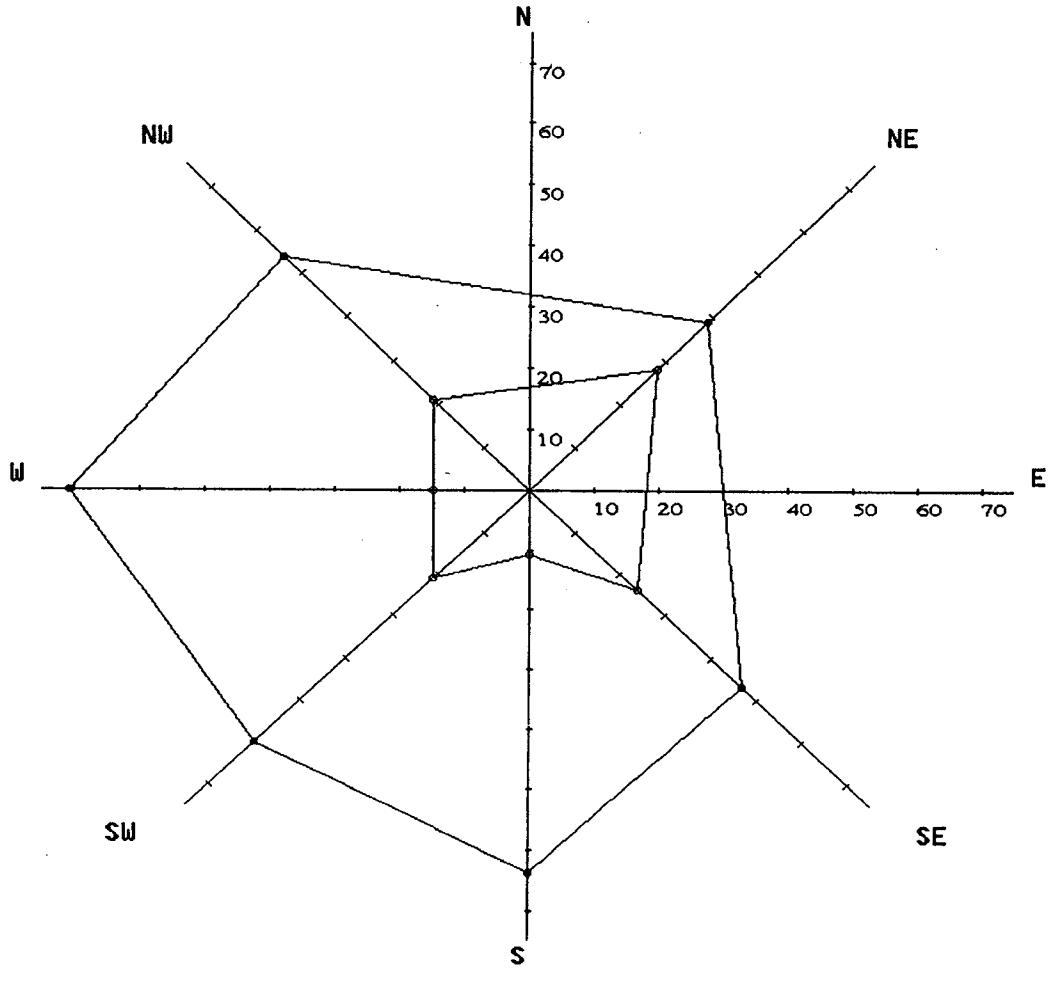

FIGURE 17(d). Wind directionality plot for Walla Walla using data from 1949-1992. [one knot is 1.92 m/s.]

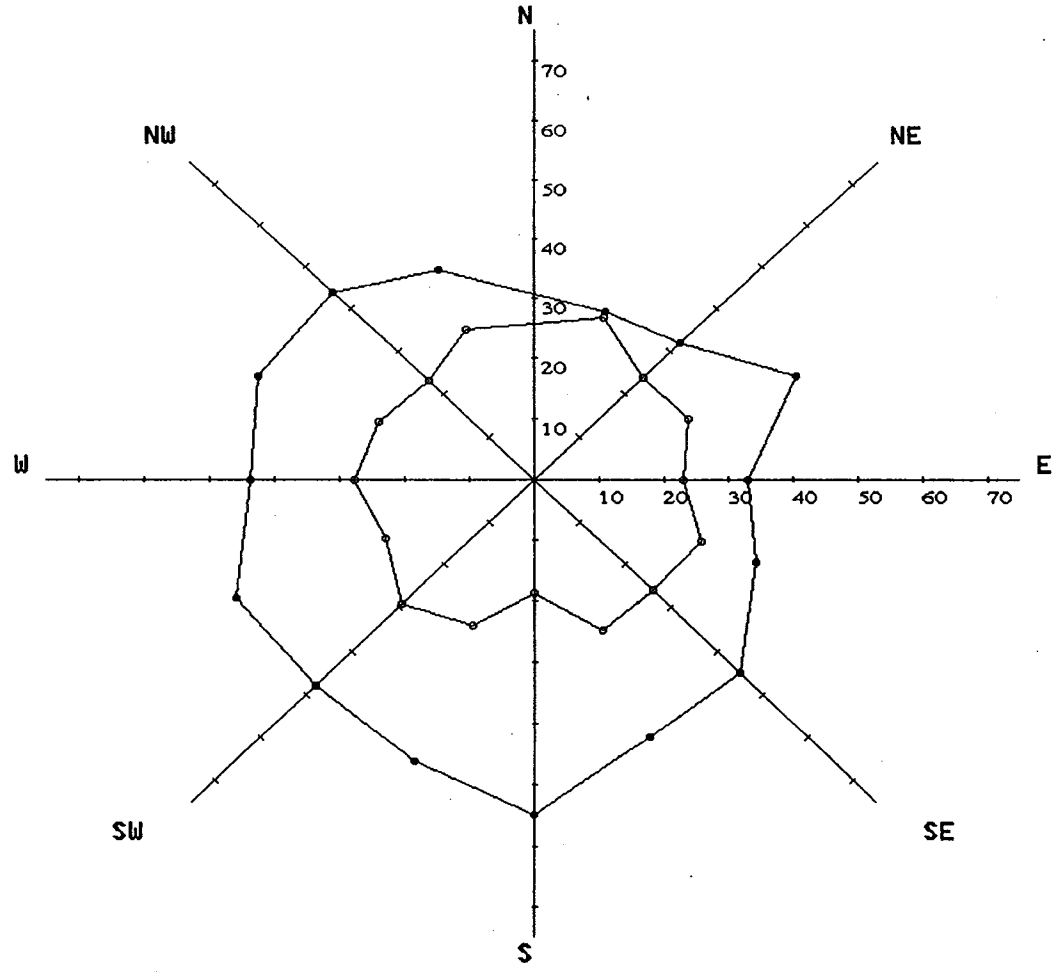

FIGURE 17(e). Wind directionality plot for Yakima using data from 1954-1992. [one knot is 1.92 m/s.]

annual intervals of the number of observations which had a particular direction and speed during the period for which data were collected. Each spoke of the rose points in the direction from which the wind blew; each indicates the relative frequency of winds of different speeds from a given direction. In Figure 18(a)-(e), for the five sites considered, the wind roses are shown. These show that winds from the South or Southwest tend to be most frequent. Olympia displays a trend towards almost uniform frequency of wind speeds across the South to West directions, whereas Seattle is a site for which the winds out of the Southwest are clearly dominant. These figures are also useful for designers in identifying for sites which directions to avoid if possible when placing signs and luminaires.

WIND PRESSURE

To a structural engineer, the pressure exerted on a structure that is induced by the flow of wind past the structure is important. The moving air possesses kinetic energy by virtue of its velocity and mass. If an obstacle is placed in the path of the wind so that the moving air is stopped or deflected from its path, then all or part of the kinetic energy of each filament of moving air is transformed into the potential energy of pressure. The intensity of pressure at any point depends on the shape of the obstacle, the angle of incidence of the wind, and the velocity and density of the air [13].

By virtue of Newton's second law, an elemental air particle in a wind flow is subjected to an inertial force proportional to its acceleration. This force is balanced by forces associated with (a) normal pressures, and (b) shear stresses caused by air viscosity. In a steady flow and in regions where shear stresses are negligible, the following relation can be obtained [14]:

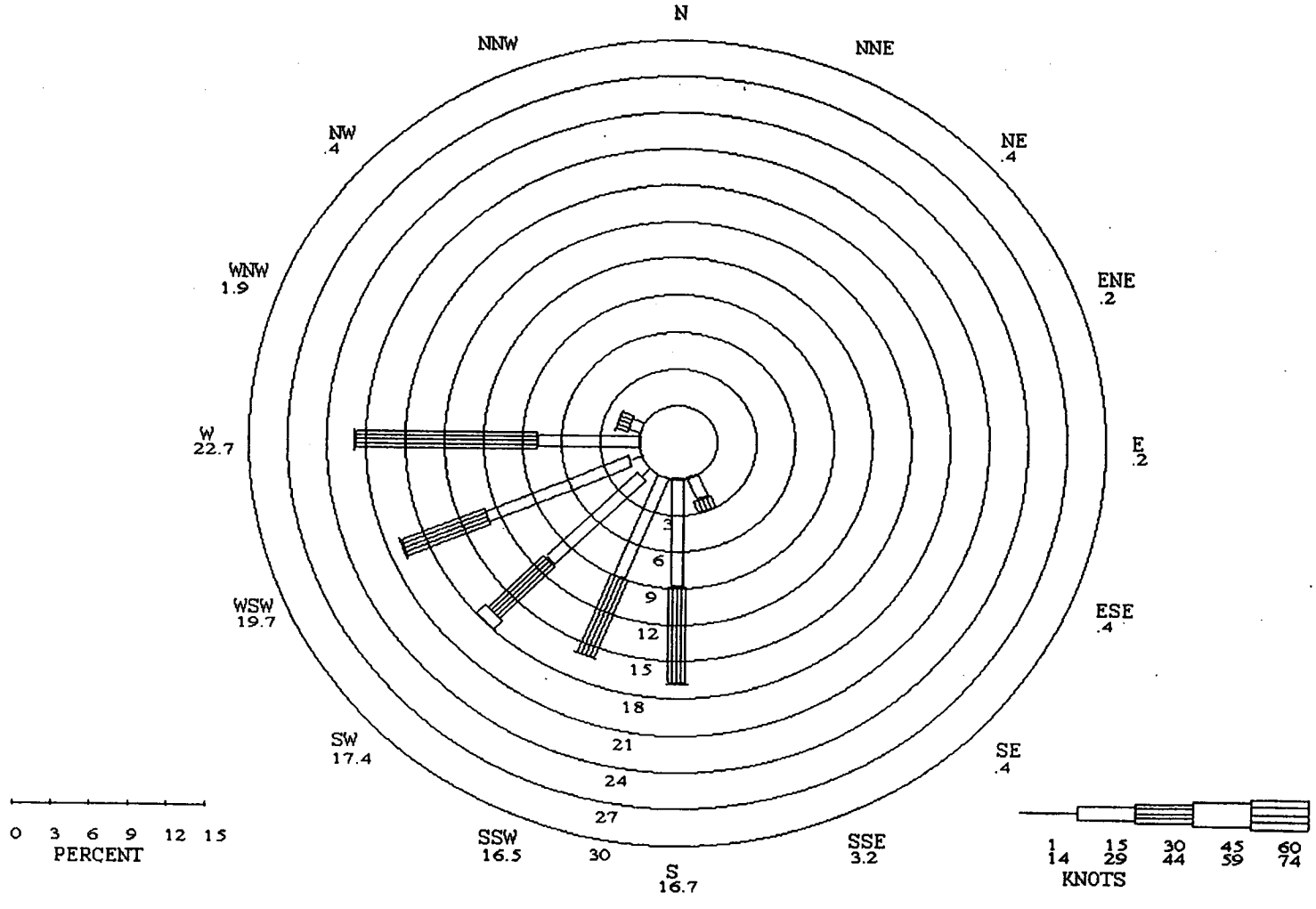

FIGURE 18(a). Wind rose for Olympia using data from 1949-1992. [one knot is 1.92 m/s.]

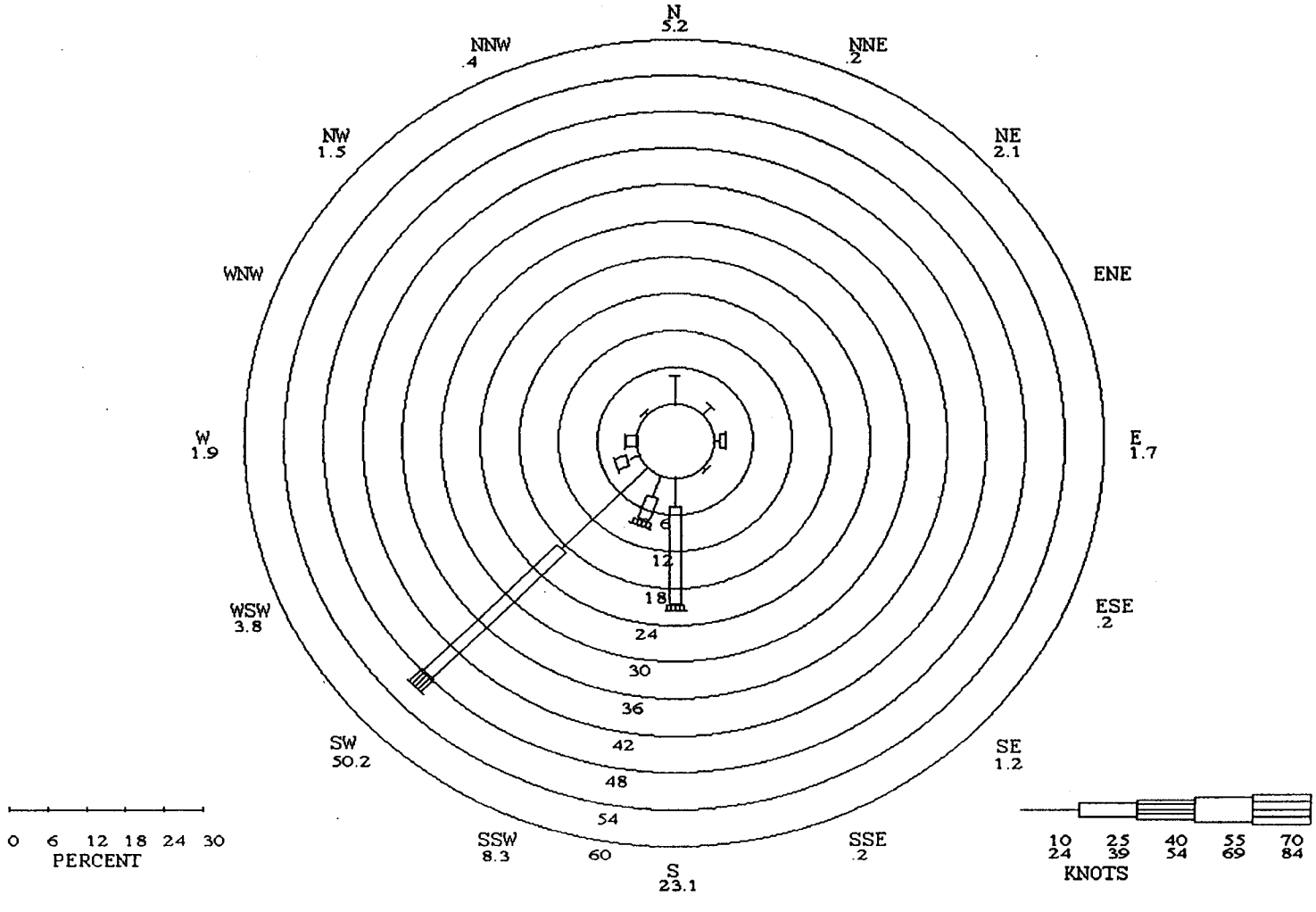

FIGURE 18(b). Wind rose for Seattle using data from 1949-1992. [one knot is 1.92 m/s.]

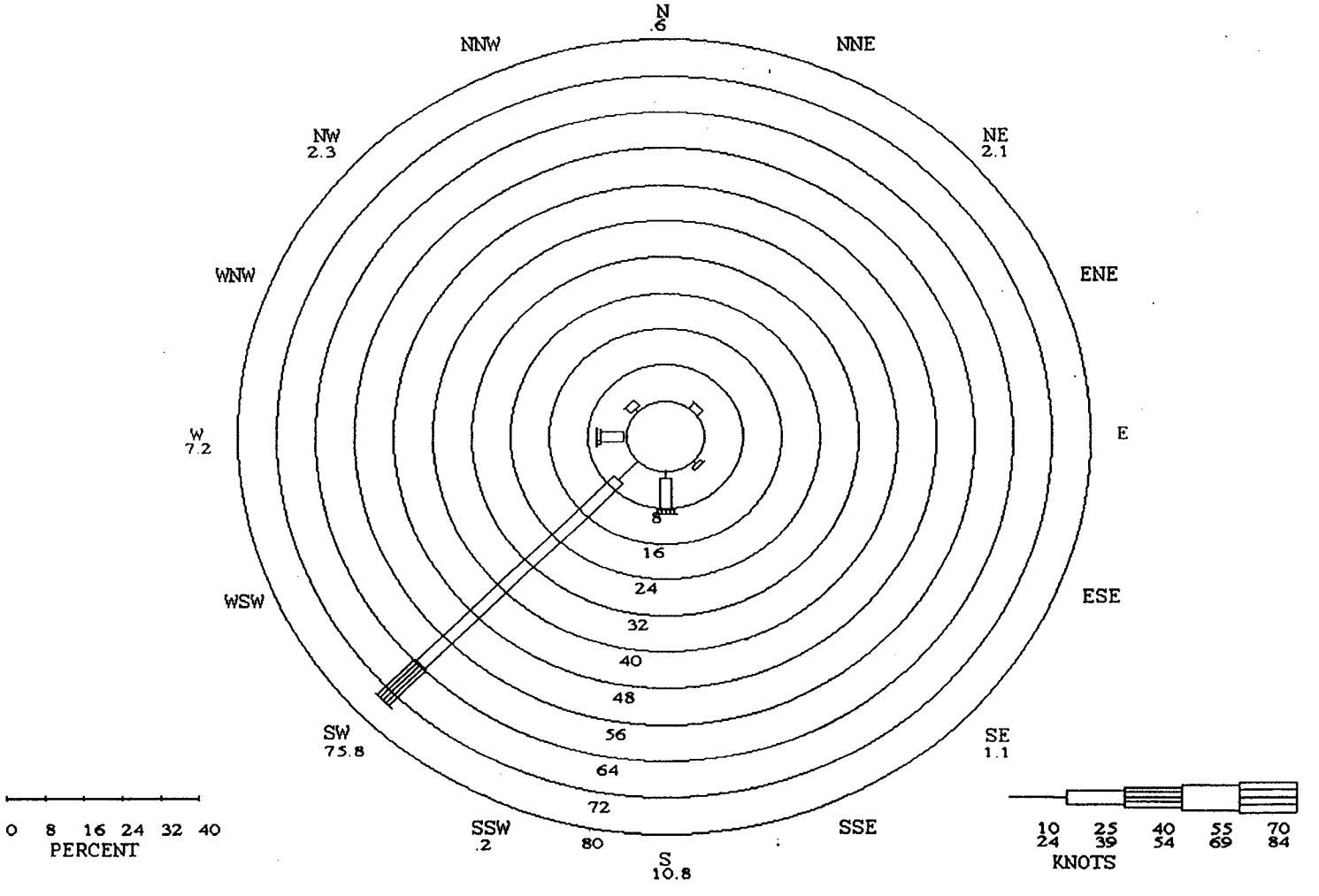

FIGURE 18(c). Wind rose for Spokane using data from 1949-1992. [one knot is 1.92 m/s.]

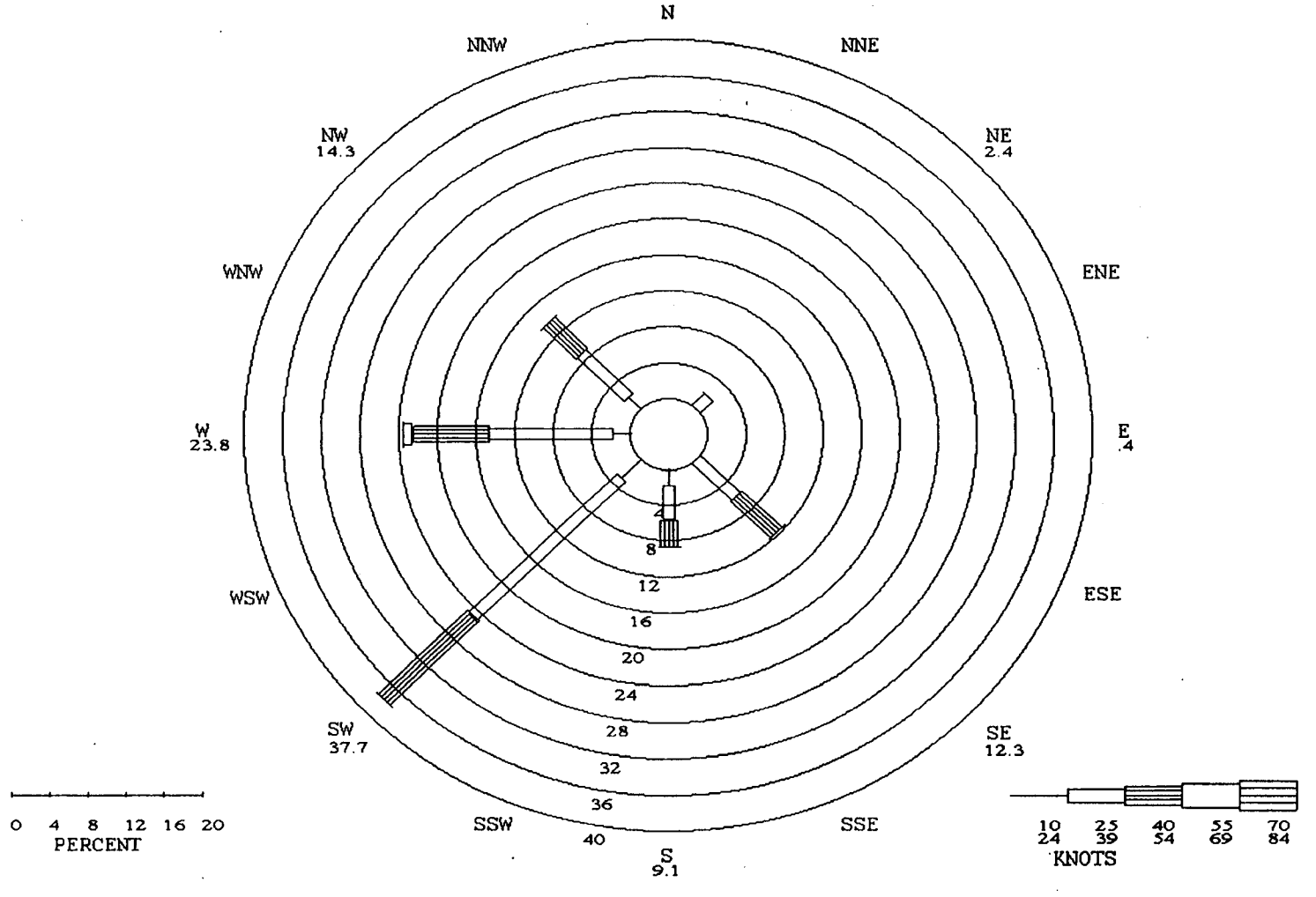

FIGURE 18(d). Wind rose for Walla Walla using data from 1949-1992. [one knot is 1.92 m/s.]

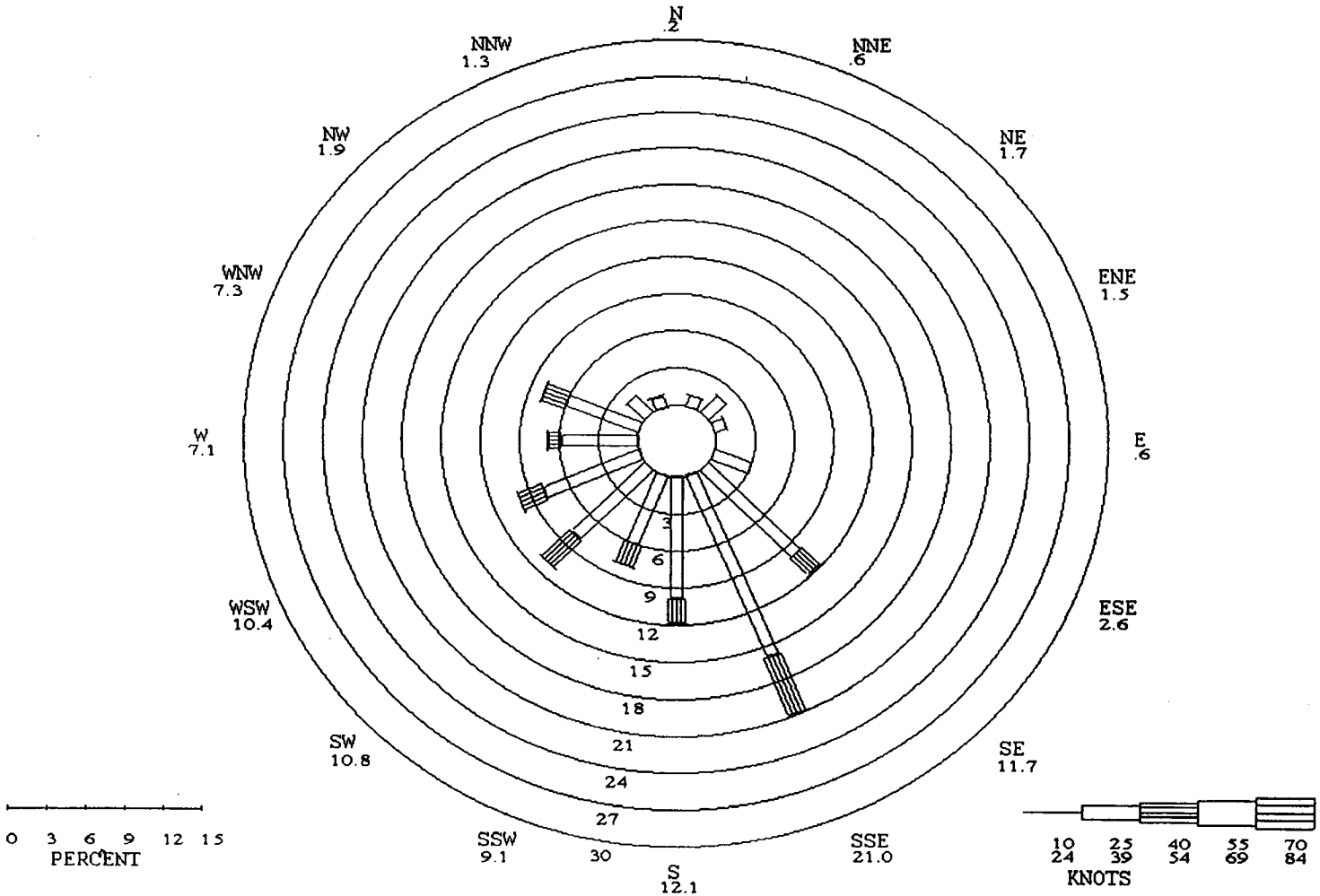

FIGURE 18(e). Wind rose for Yakima using data from 1954-1992. [one knot is 1.92 m/s.]

$$1/2\,\rho\,V^2 + p = \text{constant} \quad (17)$$

where

ρ = air density in kg/m^3

V = velocity in kmph

p = pressure in Pa

The quantity $q = 1/2\,\rho\,V^2$ has the dimension of pressure and is referred to as the dynamic pressure at the point under consideration. For standard air [1.22557 kg/m^3 (0.07651 lb/ft^3), which corresponding to 15°C and 760 mm of mercury] and velocity V expressed in kmph, the dynamic pressure in Pascals is calculated as follows [14]:

$$p = 0.0473\,V^2 \quad (18)$$

The wind pressure loading on structural supports for highway signs, signals, and luminaires is calculated below [4]:

$$P = 0.0473(1.3V)^2\,C_d\,C_h \quad [P = 0.00256(1.3V)^2\,C_d\,C_h] \quad (19)$$

where

P = wind pressure in Pa (psf)

1.3 = gust factor, G

V = fastest-mile wind speed in kmph (mph)

C_d = coefficient for drag

C_h = coefficient for height above ground

Velocity

The 1994 AASHTO design wind velocity is based on the fastest-mile wind speed at 10 m (33 ft) above the ground of terrain exposure C (defined as open field in the AASHTO specification) and annual probabilities of 0.02, 0.04, and 0.10. Wind speeds based on a 50-year mean recurrence interval or annual probability of occurrence of 0.02 are used to design luminaire support structures taller than 15.24 m (50 ft 0 in.) and for all overhead sign structures. The design of road sign structures with a relatively short life

expectancy is based on wind speeds with a mean recurrence interval of 10 years or an annual probability of 0.10. In case of failure, they do not endanger life, and they are easier to replace than overhead structures. The design of luminaire or traffic signal support structures shorter than 15.24 m is based on a wind speed a with mean recurrence interval of 25 years or an annual probability of 0.04.

The fastest-mile wind speed is defined as the fastest 1-mile stretch of wind that is measured each day at a specific site. The fastest-mile speed is averaged over the time required for a volume of air with a horizontal length of 1 mile to pass over the anemometer. Therefore, it is evident that the averaging period of the fastest-mile wind varies according to the speed of the wind. A wind with higher velocity passes the anemometer with greater speed and consequently has a smaller averaging time than a lower velocity wind. Because of these inconsistencies in the averaging time and wind speed, this is not a convenient method for professional engineers, architects, building code officials, meteorologists, news media, and the public to use to describe wind speed. In fact, the U. S. National Weather Service no longer collects fastest-mile wind speed data.

Instead, because of its convenience, 3-second gust data are now collected at a large number of stations across the United States. As the name implies, the 3-second gust wind speed is the wind speed averaged over a period of 3 seconds. The wind speed averaged over 3 seconds is recorded continuously and replaced each time the current stored value is exceeded.

It is evident from the definition that mean wind speed depends on the averaging time. Different averaging periods such as hourly, 1-minute, fastest-mile, 5-second, and 3-second have been used to represent wind speeds. For structural engineers high winds averaged over short periods are of most interest. The instantaneous velocity of wind at a given point recorded as a function of time can be represented as shown in Figure 19 [15].

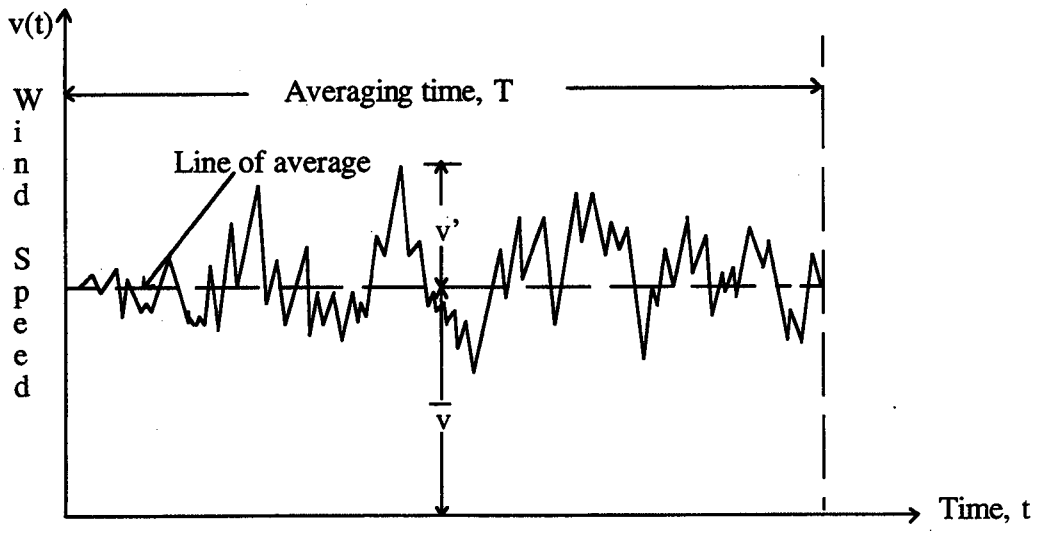

Figure 19. Typical variation of wind speed, V with time t

As the length of the averaging interval decreases, the maximum mean speed corresponding to that length increases. Therefore, the wind speed corresponding to a 3-second period will be greater than that corresponding to a fastest-mile wind, which usually varies between 20 and 60 seconds. The averaging time for the fastest-mile wind can be obtained by dividing 3600 by the fastest-mile speed. The wind speed averaged over t seconds, $V_t(z)$ [16], can be obtained from the following equation:

$$V_t(z) = V_{3600}(z)\left(1+\frac{\beta^{1/2}c(t)}{2.5\ \ln(z/z_o)}\right) \tag{20}$$

where

$V_t(z)$ = wind speed averaged over t seconds at height z in kmph (mph)

$V_{3600}(z)$ = hourly wind speed at height z in kmph (mph)

β = a constant and is assumed to be 6 for open terrain

$c(t)$ = a coefficient depending on the averaging time

z = height above ground in m (ft)

z_o = roughness length for open terrain and is assumed to be 0.05 m or (0.15 ft)

The coefficient *c(t)* was determined on the basis of statistical studies of wind speed records. The results of these studies were reported by Durst [14] and is shown in Figure 20.

Coefficient of Drag

Each point on the surface of a body experiences pressures due to the action of the airflow around the body. It is standard procedure to refer all pressures measured at a structural surface in terms of the mean dynamic pressure, $1/2\rho\ V^2$, at some reference point where the flow is undisturbed the presence of the body, where V is the mean value of the reference wind and ρ is the density of air. The pressure coefficient C_p is thus defined as the ratio of the pressure difference between local (p) and far upstream pressure (p_o) to the mean dynamic pressure.

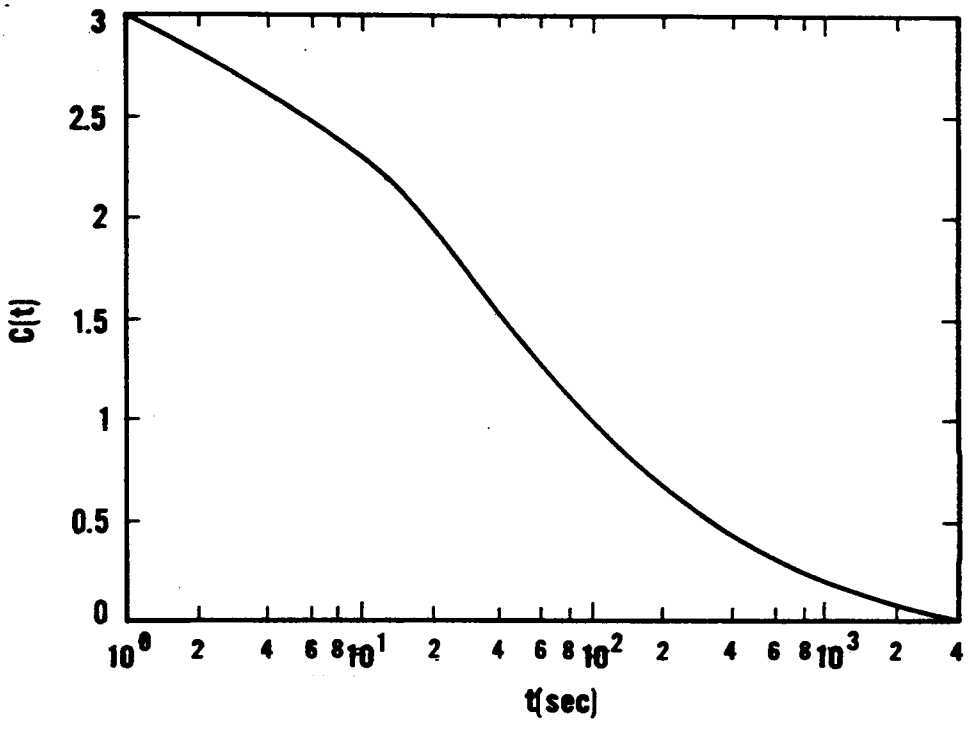

Figure 20. Dependence of the coefficient c(t) on time, t

The resultant aerodynamic force acting on the body is usually resolved into two components, one parallel and the other normal to the direction of the mean speed in the undisturbed wind flow. Figure 21 shows the drag and lift forces acting on a bluff body. Of these, the parallel component of the force is referred to as the drag or along-wind force. The drag coefficient is defined as the ratio of the drag force (D) to the product of the dynamic pressure at the reference point ($1/2\rho V^2$) and the exposed area of the bluff body [16]. Drag coefficients are usually obtained through wind tunnel tests.

The magnitude of the drag coefficient depends on (a) the geometrical form or shape of the object, (b) its orientation in the wind stream, (c) friction effects, and (d) to a limited extent, the size of the object. An object that is "streamlined" symmetrically with the direction of the wind, produces little change in the velocity of any of the elemental air particles in the wind flow; hence the principal effects from friction and the drag force would be small. On the other hand, if the object has sharp corners, greater velocity changes (separation) occur and, consequently, higher drag coefficients result. The separation of wind flow associated with different object shapes is discussed in detail in the following section.

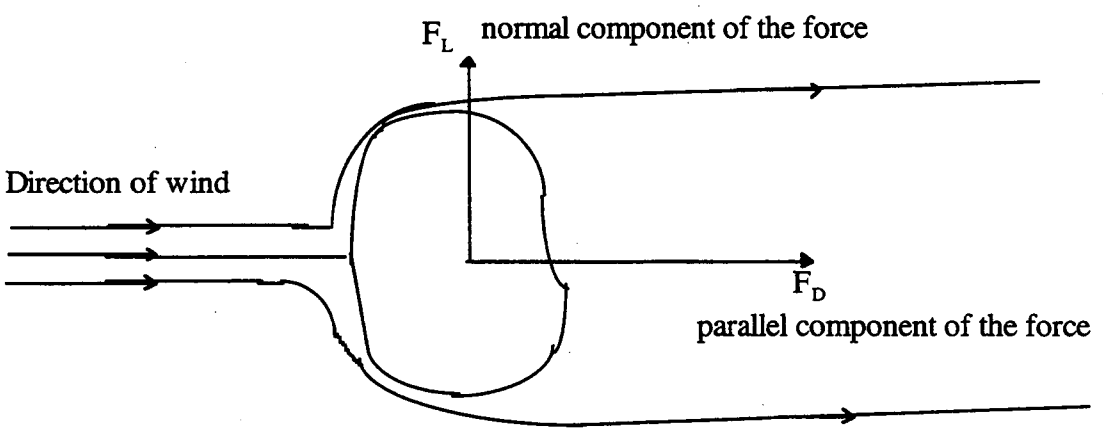

Figure 21. Drag and Lift forces acting on a bluff body [16]

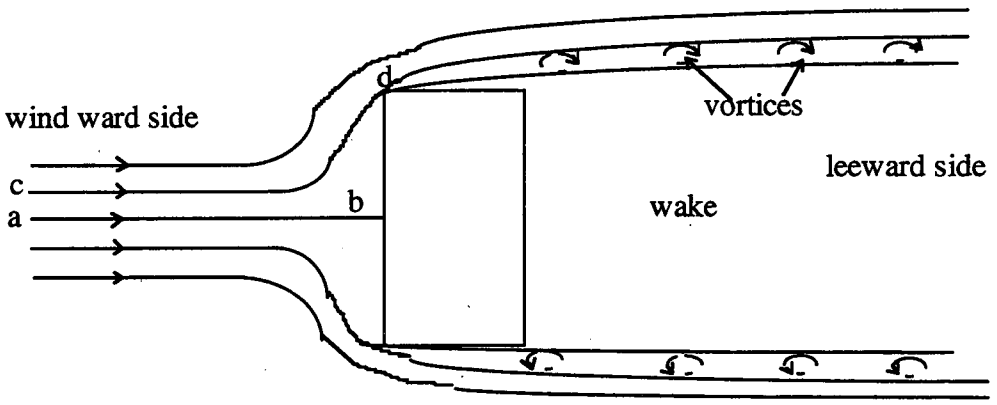

Figure 22. Flow around a bluff body with sharp corners

Separation at the Corners of Different Bluff Body Objects

Near the corners of a bluff body the air movements are highly turbulent. These regions are called "separation zones." Boundary layer separation occurs if fluid particles in the boundary layer are sufficiently decelerated by inertial forces that the flow near the surface becomes reversed. This deceleration is a result of the presence of adverse pressure gradients in the flow.

As shown in Figure 22, when the elemental air mass reaches from point "a" to "b," its velocity is reduced to zero; consequently, the pressure is higher. Throughout the windward face of the body the pressures are higher than atmospheric pressure. Therefore, positive pressures exist throughout that face. Now consider an air mass starting at point "c," where the pressure is the same as the atmospheric pressure. When it reaches point "d," the velocity increases; consequently, its pressure is reduced below atmospheric pressure. Therefore, suction or negative pressures occur at this region. Separation occurs at the corners where the pressure changes from positive to negative.

As a result of separation at sharp corners, vortices are generated that are shed into the wake flow behind the body. Such vortices can cause great suction near the separation points and at the leeward side of the body. For structures that are long in the along-wind

direction, the separation occurs at the corners and the flow reattaches after a certain distance. Upon reattachment, the pressure recovers from its low values; consequently, much less suction is encountered in the reattachment zone than in the separation zone.

The drag coefficient for certain shapes such as cylinders are Reynolds number dependent. The relation between the Reynolds number and the drag coefficient is discussed briefly in the following section.

Reynolds Number

Because air has mass, it possesses inertial forces. Viscous forces are also associated with air flow. The relation between these two can be expressed as an index of the type of flow characteristics that may be expected to occur. This index is usually the non-dimensional parameters, *Re*, known as the Reynolds number. It is defined as the ratio of the inertial force to the viscous force and is expressed as follows [16]:

$$Re = V L/\upsilon \tag{21}$$

where

V = velocity in kmph (mph)

L = surface dimension m (ft)

$\upsilon = \mu/\rho$ = kinematic viscosity

When the inertial force is greater, the Reynolds number is larger, and when the viscous force is greater, the Reynolds number is smaller.

For a circular cylinder, the drag coefficient is a function of the Reynolds number. There is a sharp drop in C_d for Reynolds numbers between $2*10^5$ and $5*10^5$. This region corresponds to the situation in which the flow around the cylinder changes from laminar to turbulent. The turbulent mixing that takes place helps transport the air with higher momentum toward the surface of the cylinder. Therefore separation occurs much farther back, and consequently the wake narrows. The relationship between the Reynolds number and C_d for a circular cylinder is shown in Figure 23 [16].

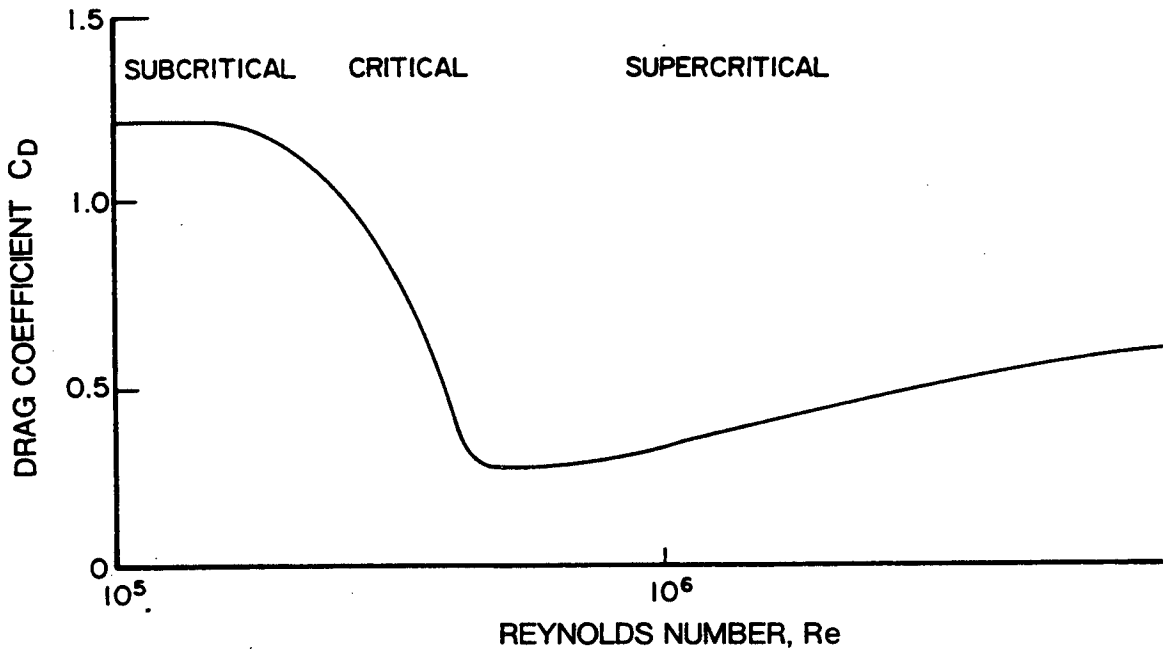

Figure 23. Variation of drag coefficient with R*e* for a circular cylinder

In the case of sharp-cornered squares, the drag coefficient is practically unchanging as the Reynolds number varies. The reason involves the early separation of the flow at the upstream corners and a lack of reattachment of the flow because of the short dimension in the along-wind direction. In the case of a rectangular body with a longer dimension in the along-wind direction, the flow reattaches; therefore, the pressure increases to atmospheric value and the wake narrows. The drag coefficient drops when the flow begins reattaching to the body. Squares with rounded corners tend to possess the same kind of critical region for the drag coefficient as circular cylinders.

Coefficient for Height Above Ground

The primary factor that affects the variation of wind velocity with height in a boundary layer is the effect of mechanical mixing of air. Therefore, only terrain roughness is important for velocity profiles. An open terrain has been used in the AASHTO specification for the design of structural supports for traffic signs, signals, and luminaires.

The adherence of the frictional force is greater near the ground, and therefore, the wind velocity is lower. As the height above ground increases, the frictional effect decreases, and consequently, the velocity is greater. Beyond gradient level, the wind flows with a gradient velocity free of frictional effect. The wind speed profile within the atmospheric boundary layer belongs to the turbulent boundary layer type, which can be approximated either by a logarithmic equation or by a power-law equation, as shown below [15]:

$$V_z = V_{10} * \ln(z/z_o)/[\ln(10/z_o)] \quad (22)$$

$$V_z = V_{10} (z/10)^{1/\alpha} \quad (23)$$

where

z = height above ground in m (ft)

z_o = roughness of ground in m

V_z = wind velocity at height z in kmph (mph)

V_{10} = wind velocity at height 10 m (33 ft) in kmph (mph)

α = a constant depending on the surface roughness

The 1994 AASHTO specification uses a value of α equal to 7 for the calculation of the coefficient for height above ground, C_h. For this part of the research, the coefficient of height C_h for the AASHTO specification was obtained by determining the ratio of velocity at a given height to velocity at 10 m (33 ft) using equations 22 and 23 (discussed in detail later in this report).

Gust Effect Factor

The gust factor, G, accounts for the effect of turbulence in the wind flow. It also accounts for along-wind loading effects due to dynamic amplification for flexible buildings and structures. It does not include allowances for across-wind loading effects, vortex shedding, instability caused by galloping or flutter, or dynamic torsional effects. For structures susceptible to loading effects that are not accounted for by the gust effect factor, the information about such effects should be obtained from wind tunnel tests. The gust response factor is a measure of the effective dynamic load produced by gusts and is intended to translate the dynamic response phenomena produced by gust loading into simpler quasi-static design criteria.

A review of the literature for the gust response factors [17] was undertaken and revealed that the gust factors for the fastest-mile wind speed are usually less than unity (between 0.83 and 1.0) and for the hourly wind speed are greater than unity (between 1.45 and 1.74), although both sets of factors result in the same loading on the structure. A similar comparison can be made between the gust response factors of the fastest-mile and 3-second gust wind speeds. The ratio of the 3-second gust speed to the fastest-mile speed is 1.2 at a height of 10 m. Therefore, the ratio of the corresponding pressures is $(1.2)^2$ or 1.44. If the slight increase of this factor with height is neglected, the gust response factor for the 3-second gust speed can be obtained by dividing the gust factor for the fastest-mile by 1.44. Table 3 shows the gust factors for the fastest-mile and 3-second gust for terrain exposure condition C.

The structural loads produced by gusts depend on structural properties such as size, natural frequency, and mechanical damping. According to proposed ASCE 7- 95, the gust effect factor should be unity for relatively rigid structures when a 3-second wind speed is used. Because gusts are localized, smaller structures are much more susceptible and thus have a larger gust factor than larger structures. Since 1959, a gust factor of 1.3

Table 3. Gust response factors for fastest-mile and 3-second gust

Height, m (ft)	G (fastest-mile)	G (3-second gust)
9.15 (30)	1.00	0.69
30.5 (100)	0.94	0.65
91.5 (300)	0.89	0.62
183 (600)	0.86	0.60
244 (800)	0.84	0.58
305 (1000)	0.83	0.58

Table 4. Wind speeds for the fastest-mile, hourly, and 3-second gust

Station	V_{fm}^{50} (10m, open) kmph (mph)	V_{hourly} kmph (mph)	V_{3s} kmph (mph)	V_{3s}/V_{fm}
Olympia	113.0 (69.9)	89.73 (55.5)	135.3 (83.7)	1.2
Quillayte	87.0 (53.8)	70.7 (43.74)	106.7 (66)	1.23
Seattle	111.2 (68.8)	88.27 (54.6)	133.2 (82.4)	1.2
Spokane	108.0 (66.8)	86.4 (53.44)	130.4 (80.64)	1.21
Walla Walla	143.2 (88.6)	112.8 (69.76)	170.2 (105.27)	1.19
Yakima	116.8 (72.25)	92.7 (57.34)	139.9 (86.53)	1.2

has been used with a fastest-mile wind speed in the AASHTO specification for the design of structural supports for traffic signs and signals.

Table 3 shows that the value of the gust effect factor for a structure at a height of 10 m is 0.69 when a 3-second gust speed is used. However for structural supports for highway signs, signals, and luminaires, a gust factor of 1.0 is recommended.

COMPARISON OF THE VELOCITY PROFILES

The primary objective of this part of the project was to compare the velocity profiles for the fastest-mile and the 3-second gust wind speeds in order to investigate the changes in the AASHTO equation [4] when a 3 second gust is used. The fastest-mile wind speeds for the six stations under consideration at a height of 10 m and a recurrence interval of 50 years are given in Table 4. The first step was the calculation of the hourly wind speed at each of the six stations from the fastest-mile wind speed. The procedure was as follows:

1. t (averaging time) $= 3600/V_{fm}$ in sec
2. Obtain V_t/V_{3600} corresponding to t sec [page 65 of Ref 16]
3. $V_{3600} = V_{hourly} = V_{fm}/(V_t/V_{360})$

The second step was the calculation of the 3-second gust speed from the fastest-mile wind speed. The 3-second gust speed at each station was calculated using equation (20) [Ref. 1, p. 65]. A value of 2.75 was used for the coefficient c(t) for a 3-second gust wind speed [14].

On the basis of equation (20), the equation for the 3-second gust wind speed can be expressed as:

$$V_{3s}(10) = V_{3600}(z)\left(1 + \frac{6^{1/2} * 2.75}{2.5 * \ln\left(\frac{10}{0.05}\right)}\right) = V_{3600}(z) * 1.509 \qquad (24)$$

The values obtained for the 3-second gust and the hourly wind speeds, along with the fastest-mile wind speed at a height of 10 m are given in Table 4. The calculations were based on a recurrence interval of 50 years.

The last column of Table 4 is included to compare the ratio of the 3-second gust speed to the fastest-mile wind speed. The values obtained were comparable to the values obtained for the proposed ASCE 7-95 (between 1.15 and 1.24) [5].

AASHTO Equation for Wind Pressure

"Wind load" refers to the pressure of the wind on the horizontal and vertical supports of signs, luminaries, and traffic signals. This pressure is calculated from equation (19), taken from the AASHTO specification [4].

Wind loads depend on many factors such as wind speed (V), averaging time of the wind speed (t), coefficient for height above ground (C_h), gust effect factor (G), and pressure coefficients (C_p). Of these, the coefficient for height and the gust effect factor are dependent on the averaging time of the wind speed and, therefore, will change when a 3- second gust is used in place of the fastest-mile wind speed.

The terrain exposure factor, K_z, in the proposed ASCE 7-95 [5] is comparable to the coefficient for height, C_h, in the AASHTO specifications [4]. When a 3-second gust is used in equation (19) instead of the fastest-mile wind speed, the parameter that changes the most is the coefficient for height above ground. AASHTO [4] uses a gust factor of 1.3 in its equation, along with the fastest-mile wind speed. A gust factor of 1.0 is proposed for use with the 3-second wind speed. To find the changes in the values of C_h, the velocity profiles of the fastest-mile and 3-second gust wind speed were compared to the hourly profiles.

Velocity Profiles

The surface of the earth exerts a horizontal drag force on moving air, which retards air flow. Thus, the velocity of the moving air (wind) decreases near the ground. But as the height above ground increases, the frictional force exerted by the earth

decreases, and therefore, wind velocity is greater. The velocity profile shows the change of velocity with height. Equations 22 and 23 were used to calculate the velocity profiles for the hourly, fastest-mile, and 3-second gust wind speeds.

ASCE 7-95 proposes to use a value of $\alpha = 9.5$ instead of 7 to make the power law exponent consistent with the 3-second gust. Therefore, for the 3-second gust velocity profile a value of $\alpha = 9.5$ was used. A value of α equal to 7 was used for the hourly profile. Sample calculations for the hourly, fastest-mile [18], and 3-second gust wind speed profiles for Olympia are given below:

Hourly profile

V_{hourly} (10 m) = 89.73 kmph (55.5 mph)

$Vz = 89.73 * (z/10)^{1/7}$ [from equation 23]

$$Vz = 89.73 * \left[\frac{\ln (z/0.05)}{\ln (10/0.05)}\right]$$ [from equation 22]

Fastest mile profile

V_{fm} (10 m) = 113.0 kmph (69.9 mph)

$$Vz = \left[\frac{V_{fm}(10) * V_{hourly}(z)}{V_{hourly}(10)}\right] * \frac{1}{\left(1 + \frac{z-10}{10} * 0.02\right)}$$ [Reference 18] (25)

3-second gust profile

V_{3s} (10 m) = 135.3 kmph (83.7 mph)

$Vz = 135.3 * (z/10)^{1/9.5}$ [from equation 23]

$$Vz = 135.3 * \left[\frac{\ln (z/0.05)}{\ln (10/0.05)}\right]$$ [from equation 22]

The value of z for open terrain may increase up to z_g = 289.6 m (950 ft). However, the structural supports for traffic signs and signals are not usually as tall as 950 ft. Therefore, values of z up to 91.4 m (300 ft) were used to correspond to the AASHTO-94 values.

The velocity profiles for the hourly, fastest-mile, and 3-second gust wind speeds for Olympia are shown in figures 24 and 25. The coefficient C_h was then calculated in each case by dividing V_z (velocity at height z) by V_{10} (velocity at height 10 m). The C_h values obtained from the power law and logarithmic profiles, along with the 1994 AASHTO values, are given in Table 5. Because the velocity profiles were similar and the values of C_h obtained in each case were all the same for the six stations, only the values for one station (Olympia) are shown.

Table 5 shows that, in order to find a relationship between the calculated C_h values obtained from the hourly profile for α equal to 7 (power law) and the C_h values in the AASHTO Specification, which is based on a value of α equal to 7, a linear regression analysis had to be performed. This is shown in Figure 24. The result of the regression analysis was the following equation:

$$y = 1.6476\,x - 0.6472 \tag{26}$$

where x is the C_h values obtained from the hourly profile and y is the C_h values corresponding to the AASHTO Specification [4]. The above equation was then used to convert the values of C_h for the 3-second gust to the corresponding new AASHTO values. The calculated values from the profiles and the values obtained using equation 26 are given in Table 6. The values obtained using the equation for the case of $\alpha = 7$ should be similar to the AASHTO (1994) values.

The values in column 4 of Table 6 are the proposed C_h values for use in the AASHTO specification. These values reflect the changes in C_h when a 3-second gust wind speed is used instead of the fastest-mile wind speed. Values in column 7 represent the ratio of the proposed C_h values to the old C_h values for the AASHTO specification and were obtained by dividing the values in column 4 by the values in column 6. To compare the proposed and existing equations for the calculation of pressure (equation 19), the following steps were adopted.

Table 5. Coefficient for height, C_h calculated from the velocity profiles

Height m (ft)	C_h						
	Hourly		Fastest-mile		3-second gust		AASHTO (94)
	power	log	power	log	power	log	
0 < H < 4.27 (0 < H < 14)	0.89	0.84	0.90	0.85	0.91	0.84	0.80
4.27 < H < 8.84 (14 < H < 29)	0.98	0.98	0.98	0.98	0.99	0.98	1.00
8.84 < H < 14.94 (29 < H < 49)	1.06	1.08	1.05	1.07	1.04	1.08	1.10
14.94 < H < 30.18 (49 < H < 99)	1.17	1.21	1.13	1.16	1.12	1.21	1.25
30.18 < H < 45.42 (99 < H < 149)	1.24	1.29	1.16	1.20	1.17	1.29	1.40
45.42 < H < 60.66 (149 < H < 199)	1.29	1.34	1.17	1.22	1.21	1.34	1.50
60.66 < H < 91.14 (199 < H < 299)	1.37	1.42	1.18	1.22	1.26	1.42	1.60

Table 6. C_h converted to get the corresponding new AASHTO values

Height m (ft)	C_h from velocity profiles		C_h converted to correspond to AASHTO values		C_h for AASHTO	$\frac{C_{hn}}{C_{ho}}$
	$\alpha = 9.5$	$\alpha = 7$	$\alpha = 9.5$	$\alpha = 7$	1994, $\alpha = 7$	
0 < H < 4.27 (0 < H < 14)	0.91	0.89	0.85	0.82	0.80	1.06
4.27 < H < 8.84 (14 < H < 29)	0.99	0.98	0.98	0.97	1.00	0.98
8.84 < H < 14.94 (29 < H < 49)	1.04	1.06	1.07	1.10	1.10	0.97
14.94 < H < 30.18 (49 < H < 99)	1.12	1.17	1.20	1.28	1.25	0.96
30.18 < H < 45.42 (99 < H < 149)	1.17	1.24	1.28	1.40	1.40	0.91
45.42 < H < 60.66 (149 < H < 199)	1.21	1.29	1.35	1.48	1.50	0.90
60.66 < H < 91.14 (199 < H < 299)	1.26	1.37	1.43	1.61	1.60	0.89

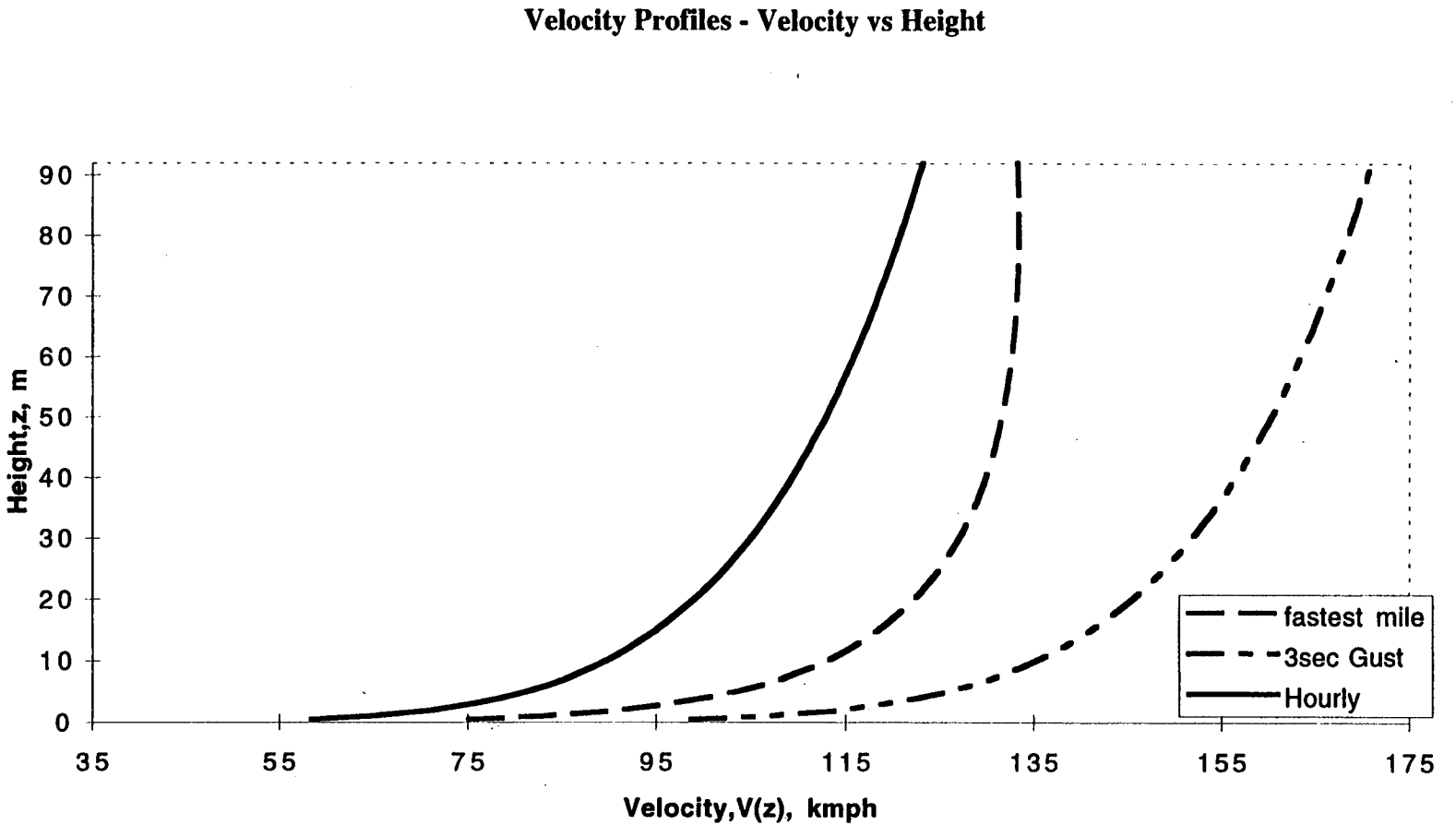

Figure 24. Velocity Profiles for Hourly, Fastest-mile, and 3-second gust wind speeds using Power Law

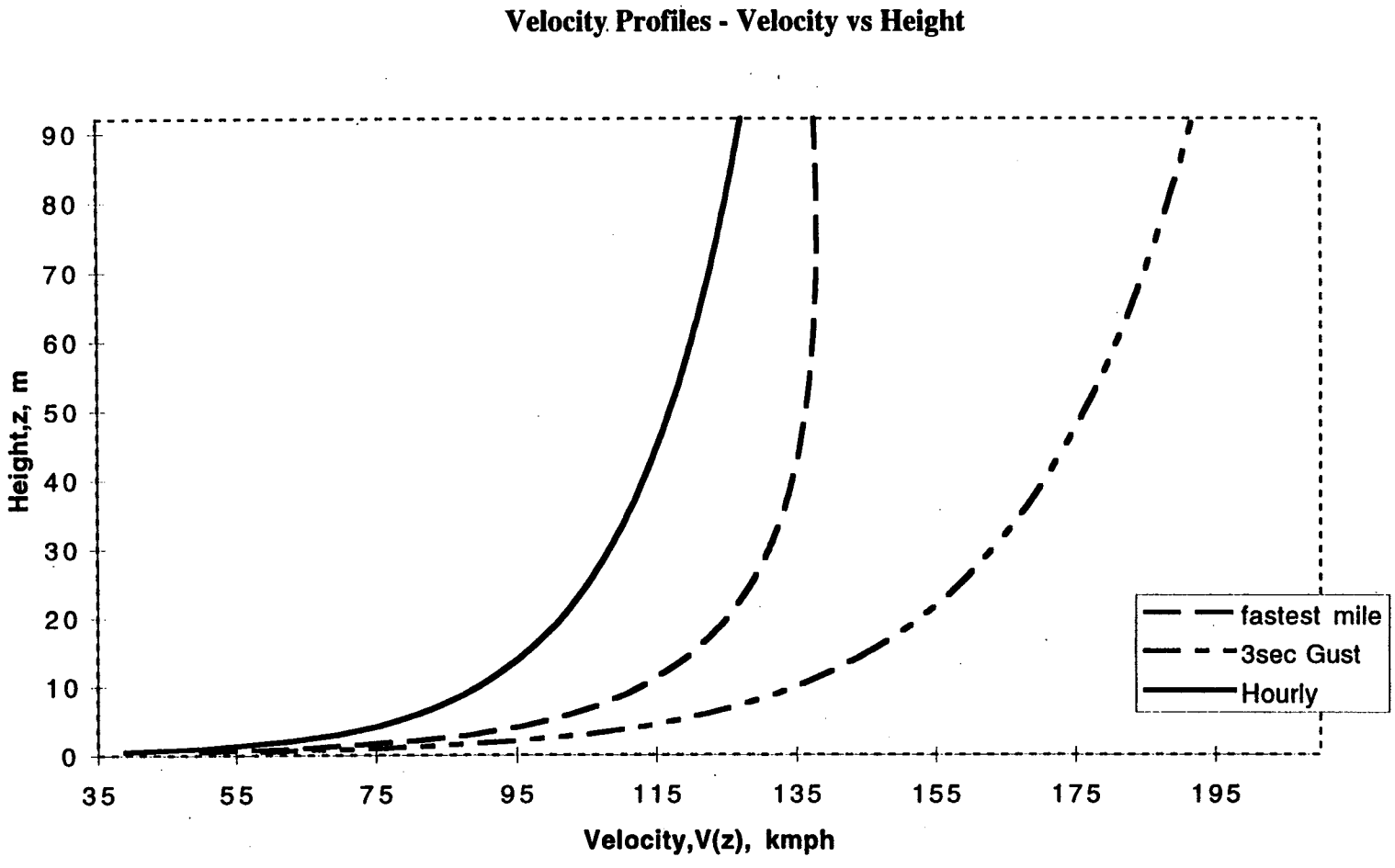

Figure 25. Velocity Profiles for Hourly, Fastest-mile, and 3-second gust wind speeds using Log. Law

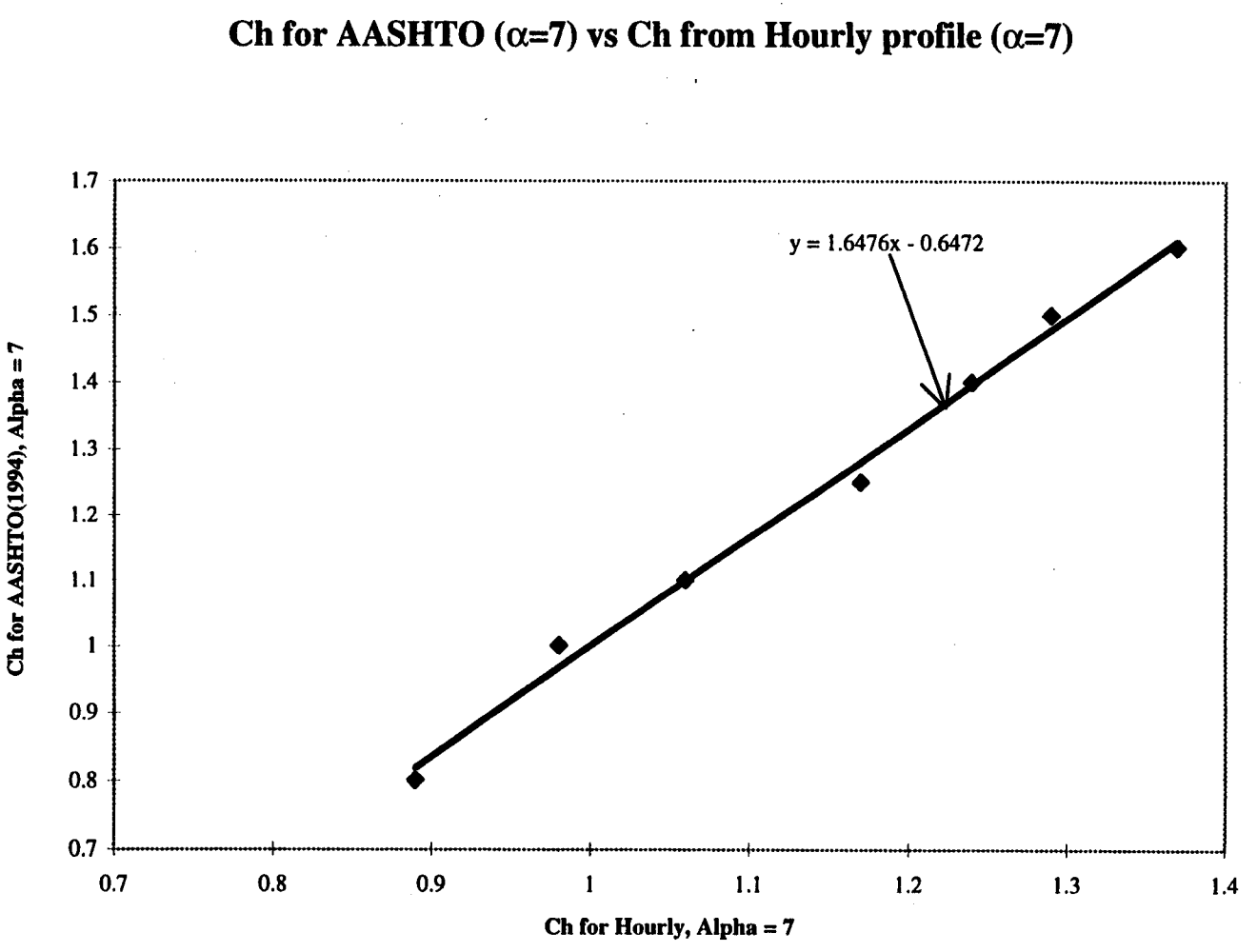

Figure 26. Relation between Ch from AASHTO[4] and the Ch obtained from the Hourly profile

The 1994 AASHTO equation is

$$P_o = 0.0473(1.3\ V_{fm})^2\ C_{do}\ C_{ho} \qquad [P_o = 0.00256\ (1.3\ V_{fm})^2\ C_{do}\ C_{ho}] \qquad (27)$$

The new equation for pressure when using a 3-second gust wind speed is

$$P_n = 0.0473\ (G\ V_{3s})^2\ C_{dn}\ C_{hn} \qquad [P_n = 0.00256\ (G\ V_{3s})^2\ C_{dn}\ C_{hn}] \qquad (28)$$

where C_{do}, C_{ho}, C_{dn}, and C_{hn} represent the old and new values of the drag coefficients and coefficients for height above ground, respectively.

The drag coefficient was assumed to be the same in both cases. The velocity for the 3-second gust wind speed can be very closely approximated as 1.2 times the fastest-mile wind speed. A gust factor of G equal to 1.0 was recommended to use with the 3-second gust wind speed. Therefore, the new equation for pressure is

$$P_n = 0.0473\ (1.0*1.2\ V_{fm})^2\ C_{do}\ C_{hn} \quad [P_n = 0.00256\ (1.0*1.2\ V_{fm})^2\ C_{do}\ C_{hn}] \qquad (29)$$

To keep the pressure the same for the old and new provisions, Pn/Po was assumed to equal 1; that is,

$$P_n/P_o = 1 = \frac{0.0473\ (1.0*1.2\,V_{fm})^2\,C_{do}\ C_{ho}}{0.0473\ (1.3\ V_{fm})^2\,C_{do}\ C_{ho}} = \frac{1.2^2\,C_{hn}}{1.3^2\,C_{ho}} \qquad (30)$$

That is, $C_{hn}/C_{ho} = 1.17$

The last column of Table 6 shows the values of C_{hn}/C_{ho} obtained for different heights. As indicated above, if the pressures are to remain the same, the ratio of C_{hn}/C_{ho} should be 1.17. The values of C_{hn}/C_{ho}, calculated from the velocity profiles shown in Table 6 vary from 0.89 to 1.06. These values are slightly lower than 1.17, but they are comparable.

CONCLUSIONS

The first part of this project focused on identifying the temperature microclimate patterns of Washington State and developing an isothermal map for the effective composite bridge temperature values. Equations obtained from the 2-D heat transfer analysis by Moorty [2] were used to convert the ambient air temperatures at each station to the corresponding mean bridge temperature values. Moorty found that the measured bridge temperatures and the temperatures obtained by the heat transfer analysis were similar. Furthermore, the measured movements and the movements obtained by the analysis were similar. This meant that the equations obtained by Moorty's heat transfer analysis to predict the bridge temperatures from the ambient air temperatures were reasonable to apply in this research.

The maps of maximum, minimum, and range of air temperatures clearly show the different temperature patterns of Washington State. The air temperature ranges vary considerably from 51°C to 85°C between the western and eastern regions of the state. The AASHTO specifications for composite (or steel) bridges recommend only two ranges. To accurately predict the bridge movements caused by temperature at a location, one must know the temperature patterns of that particular location. That is why the isothermal map (Figure 11) developed in this research will be very useful in accurately predicting temperature changes in composite bridges at different locations. This map yields mean bridge temperature range values between 46°C and 90°C.

Figure 7 shows that more than half of the stations under consideration fall outside of the temperature range values specified by AASHTO. It also reveals that the majority of the stations falling below this range are in the western half of the state. Therefore, in this region the thermal changes could be over-estimated if the AASHTO values are used, and allowance for unnecessary movement can result in unnecessarily high bridge construction costs. By using Figure 11 with the AASHTO specification, WSDOT can

avoid the unnecessary construction costs related to expansion joints and bearings in the western half of Washington State. Figure 7 also reveals that the eastern half of Washington State falls within the AASHTO range. The effect of elevation on air temperatures was also a consideration, and a detailed study revealed that not only elevation, but also other factors such as latitude and closeness to the ocean, affect the temperature of a region.

The second part of the project focused on incorporating a 3-second wind speed into the AASHTO (1994) specification [14] for calculating pressure on structural supports. It also focused on determining the extreme wind probability values for six stations across Washington State. When a 3-second gust wind speed was used in equation 19, the resulting pressure obtained would be greater because the 3-second speed is greater than the fastest-mile wind speed. To keep the pressure the same, other parameters associated with the equation were adjusted on the basis of an investigation of velocity profiles and the gust factor. Because the effect of using a greater wind speed had only a small effect on the drag coefficient, it was assumed to be the same.

The velocity profiles for the hourly, fastest-mile, and 3-second gust wind speeds were developed on the basis of power and logarithmic laws. The calculation of the coefficient for height above ground was based on these profiles and obtained by dividing the velocity at height z by the velocity at a height of 10 m. Tables 5 and 6 show the values of C_h obtained in each case and the values of new C_h corresponding to the AASHTO equation. A comparison of the proposed (new) and the existing (old) AASHTO equations based on the C_h values was also presented The values of C_hn/C_ho obtained from the velocity profiles (column 7 of Table 6) were slightly smaller than the value of C_hn/C_ho (1.17) obtained from the comparison of the old and new equations. These differences were reasonable, given the fact that the drag coefficient was assumed to be the same in both cases. The values of C_h in column 4 of Table 6 represent the proposed C_h values, which can be adopted by AASHTO to use with a 3-second gust wind speed.

RECOMMENDATIONS

Verification of the temperature values in the isothermal map by the field measurement of bridge temperatures is recommended. The methodology for identifying appropriate temperatures ranges to be used in conjunction with the AASHTO specification developed by Moorty [2] has been greatly expanded in the present study. This methodology is recommended for use by WSDOT in assessing thermal stresses in bridge design.

The isothermal map developed in this project will be helpful only to determine the temperature changes in composite bridges that have a concrete deck over steel girders. Similar maps can be obtained through further analysis and investigation for other bridge types such as curved bridges, box girder bridges, or concrete T- girder bridges, building upon Moorty's original study [2].

The wind directionality and rose maps for the seven sites suggest that winds out of the southwest quadrant are strongest in the western half of the state. The effect of using a 3-second gust wind speed on the drag coefficient needs to be further investigated through wind tunnel tests on certain structural shapes for which the drag coefficient is sensitive to the Reynolds number.

The lessening effect of gust winds above a height of 10 m also needs to be further studied so that a more accurate gust factor can be incorporated.

REFERENCES

1. American Association of State Highway and Transportation Officials (AASHTO), 1994, "Standard Specification for Highway Bridges."

2. Moorty, S., "Thermal Movements in Bridges", PhD thesis, University of Washington, Department of Civil Engineering, 1991.

3. MapInfo Corporation, MapInfo Reference Manual, Desktop Mapping Software, Troy New York, 1993.

4. American Association of State Highway and Transportation Officials, "Standard Specification for Structural Supports for Highway signs, Luminaires, and Traffic Signals," Washington D. C., 1994.

5. Proposed Wind Load Provisions of ASCE 7-95.

6. Elbadry, M. M., and Ghali, A., "Temperature Variations in Concrete Bridges," Journal of Structural Engineering, vol. 109, No. 10, October, 1983, pp. 2355 - 2374.

7. Emanuel, J. H., and Hulsey, J. L., "Temperature Distributions in Composite Bridges," Journal of the Structural Division, ASCE, vol. 104, No. ST1, January, 1978, pp. 65 -77.

8. Radolli, M., Dillon, M. M., and Green, R., "Thermal Stress Analysis of Concrete Bridge Super structures," Transportation Research Record, vol. 607, 1976.

9. Demars, M., "Development of a Contour Temperature Map for Design of Thermal Movements in Composite Bridges," Masters thesis, University of Washington, Department of Civil Engineering, 1994.

10. Fu, H. C., Ng, S. F., and Cheung, M. S., "Thermal Behavior of Composite Bridges," Journal of Structural Engineering, vol. 116, No. 12, December, 1990, pp. 3302 - 3323.

11. Reynolds, J. C., and Emanuel, J. H., "Thermal Stresses and Movements in Bridges," Journal of the Structural Division, ASCE, vol. 100, No. ST1, January, 1974, pp. 63 -77.

12. Thom, H. C. S., "New Distributions of Extreme Winds in the United States," Journal of the Structural Division, ASCE, vol. 94, No. ST7, July, 1968, pp. 1787 - 1801.

13. Task Committee on Wind Forces, "Wind Forces on Structures," American Society of Civil Engineers, Transactions, vol. 126, part II, 1961, Paper No.3269, pp. 1124 - 1198.

14. American Society of Civil Engineers, "Wind Loading and Wind Induced Structural Response," A State of the Art Report prepared by the Committee on Wind Effects, 1987.

15. Liu, H., *Wind Engineering*, A Hand Book for Structural Engineers, University of Missouri - Columbia, 1991, Prentice Hall, Englewood Cliffs, New Jersey 07632.

16. Simiu, E., and Scanlan, R. H., *Wind Effects on Structures*, Second edition, John Wiley and Sons, New York, 1986.

17. Vellozzi, J., and Cohen, E., "Gust Response Factors," Journal of the Structural Division, ASCE, vol. 94, No. ST6, June, 1968, pp. 1295 - 1313.

18. Simiu, E., Changery, M. J., and Filliben, J. J., "Extreme Wind Speeds at 129 Stations in the Contiguous United States," National Bureau of Standards Building Science Series 118, March 1979.

APPENDIX A

OUTLINE OF MOORTY'S HEAT TRANSFER ANALYSIS AND DETERMINATION OF MEAN BRIDGE TEMPERATURES

APPENDIX A

OUTLINE OF MOORTY'S HEAT TRANSFER ANALYSIS AND DETERMINATION OF MEAN BRIDGE TEMPERATURES

Temperature variations in bridges are mainly influenced by solar radiation, ambient air temperature, and wind speed. Numerous methods have been developed by different researchers to predict the temperature variations in bridges given these environmental factors.

Usually weather stations record the daily ambient air temperatures and wind speed, but very few stations record solar radiation. Moorty [2] studied and compared the various methods available for the calculation of solar radiation and found that the best fit was provided by Potgeiter's method. Moorty [2] explains a detailed theoretical method in her report to calculate the solar radiation on the basis of several factors such as the latitude, hour angle, the declination angle, solar zenith angle, altitude angle, and the solar azimuth angle.

Ambient air temperature data are available in most of the U.S. locations for daily maximum and minimum values. In locations where the hourly temperatures were not available, a sine curve was used to interpolate the hourly values between the maximum and minimum values [10]. The equation is

$$T_a = 1/2(T_{max} + T_{min}) + 1/2(T_{max} - T_{min}) \sin[(t - 9)\pi/12] \quad \text{(A-1)}$$

Wind affects the convective heat transfer and has been found to influence the temperature variations in bridges considerably. Higher wind speeds reduce the temperature of bridge surfaces to values close to ambient air temperatures. Moorty [2] assumed an average wind speed of 8 mph in her analysis.

Because many empirical equations have been proposed by different researchers for heat transfer coefficients, Moorty conducted an investigation to determine the most

appropriate equation to use in the heat transfer analysis [2]. Moorty proposed the following equation for calculating the total heat transfer coefficient at the top of the deck.

$$h = 13.5 + 3.88\,u, \ W/m^2\,^{\circ}C \qquad \text{(A-2)}$$

where u is the wind speed in m/s. A value of half of that was used at the bottom. Moorty used the heat transfer coefficient obtained from the above equation and the solar radiation obtained by the theoretical method for the boundary conditions in her 1-D and 2-D heat transfer analyses.

Moorty [2] modeled the three most widely used highway bridge types: (1) concrete T-beam bridge, (2) composite (concrete deck over steel girders) bridge, and (3) concrete box girder bridge. The present project was focused on the analysis of composite (concrete deck over steel girder) bridges because steel is more sensitive to temperature than concrete. Relationships for the two other bridge types investigated by Moorty may be analyzed in a similar manner [2, pp.47-48]. Moorty stated an accuracy of approximately 2 °C. Concrete bridges, which have a higher thermal mass, respond to the temperature changes more slowly. The 2-D heat equation can be further simplified to a 1-D equation for composite bridges because the heat loss along the sides is accounted for by the rapid response of steel to the changes in ambient air temperature [9]. The resulting 1-D equation given below assumes that the temperature variation along the length and width of the bridge is constant.

$$\rho\, c \frac{\partial T}{\partial t} = k \frac{\partial^2 T}{\partial x^2} \qquad \text{(A-3)}$$

The temperature distributions obtained by the 2-D and 1-D analyses were the same for composite bridges because the steel beams are thin and have high conductivity and therefore, the temperature in the girders is mainly influenced by the ambient air temperature. The top of the steel girders has the same temperature as the bottom of the concrete deck and the temperature increases (in summer) or decreases (in winter)

linearly, to the top. Below the deck the steel girder is at a constant temperature equal to the ambient temperature.

Mean Bridge Temperature Equations

Moorty [2] established an overall temperature from the temperature gradients, and by using this temperature, the longitudinal expansion of the bridge can be determined. This longitudinal movement is the primary concern for the design of a bridge. The longitudinal expansion, then can be obtained using the equation specified by AASHTO [1]:

$$\Delta_T = \alpha L \Delta T \qquad \text{(A-4)}$$

where

Δ_T = longitudinal expansion in m

α = coefficient of thermal expansion in m/m/°C

L = length of the structure in m, and

ΔT = temperature range in °C

The "overall" temperature obtained from the temperature gradient is known as the "mean bridge temperature," which governs the longitudinal movement of the bridge deck. The mean bridge temperature is a weighted mean of temperatures in the bridge. The mean bridge temperature is obtained by summing the products of areas between isotherms and their mean temperatures and then dividing by the total area of cross-section of the bridge deck. The equation is given below [2]:

$$\theta_m = \frac{\sum A_i E_i \alpha_i \theta_i}{\sum A_i E_i \alpha_i} \qquad \text{(A-5)}$$

where

θ_m = mean bridge temperature in °C

A_i = cross section area of the slice considered in m^2

E_i = modulus of elasticity in MPa

α_i = coefficient of thermal expansion in m/m/$^{\circ}$C

θ_i = temperature between two isotherms in $^{\circ}$C

Equation A-5 was based on the condition that the sum of induced expansion and contraction forces across the section equal zero [9]. To determine the thermal movements from non-uniform temperature variations, a weighted average of the temperature isotherms at different levels through a vertical section of the bridge deck is used.

To compare the temperature ranges specified by AASHTO, Moorty [2] modeled the three bridge types—T-beam bridge, composite steel girder bridge, and concrete box girder bridge—and analytically predicted the temperature ranges by considering measurements from stations in different parts of the United States. For the analysis, she chose eleven stations across U.S and considered the maximum and minimum temperatures for the days of interest. Those stations and the maximum and minimum temperatures obtained at each station are shown in Table A-1 [2]. The days selected for the analysis were the days on which the maximum and minimum temperatures had occurred for the past 50 years. Then heat transfer analysis was undertaken for each station in summer and winter to obtain the maximum and minimum mean bridge temperatures, respectively. Moorty's analysis included a period of four days to eliminate the response lag of the bridge to environmental changes and the effect of the initial conditions. The wind speeds for the stations varied between 6 and 8 mph in summer and between 7 and 9 mph in winter. Because wind speed has little correlation with solar radiation and ambient temperature, Moorty assumed a constant wind speed of 7 mph in summer and a speed of 8 mph in winter. The material properties used for the analysis of the composite bridge are shown in Table A-2 [2].

The maximum and minimum mean bridge temperatures were then obtained using the heat transfer analysis for all four days considered. Table A-1 shows the eleven stations selected for the analysis; the maximum, minimum, and range of ambient air temperature values; and the maximum, minimum, and range of mean bridge values.

Table A-1. Air and bridge temperature values used for Moorty's analysis [2]

Station	Ambient Air Temperature (°C)			Ambient Air Temperature (°C)		
	Max.	Min.	Range	Max.	Min.	Range
Valdez, Alaska	25.60	-26.7	52.30	29.70	-22.10	51.80
Phoenix, Arizona	46.50	-4.20	50.70	51.30	1.70	49.60
Fresno, California	43.00	-5.80	48.80	47.30	0.00	47.30
Apalachicola, Florida	36.00	-5.80	41.80	41.10	0.60	40.50
Great Falls, Montana	35.60	-35.6	71.20	40.00	-32.20	72.20
Albuquerque, New Mexico	39.60	-25.0	64.60	44.40	-20.10	64.50
Columbia, Missouri	46.00	-20.0	66.00	50.20	-15.20	65.40
Cape Hatteras, N. Carolina	31.80	-3.90	35.70	36.50	1.70	34.80
Fort Worth, Texas	44.30	-10.6	54.90	49.40	-5.70	55.10
Seattle, Washington	34.40	-15.0	49.40	38.80	-10.00	48.80
Reno, Nevada	39.40	-23.3	62.70	42.60	-16.10	58.70

Table A-2 Material properties used for the composite bridge [2]

	density, kg/m^3 ($lb\ m/ft^3$)	spec. heat, J/kg K (Btu/lb m)	conductivity, W/m K (Btu/hr ft F)	absorptivity
Concrete	2402.78 (150)	950.404 (0.227)	1.4 (0.809)	0.65
Steel	7752.95 (484)	485.669 (0.116)	35.999 (20.8)	0.65

Using these results, Moorty obtained relationships between the ambient air temperatures and the mean bridge temperatures by means of linear regression analyses [2]. The relationship between maximum ambient air temperature and maximum mean bridge temperature obtained by the analysis is

$$\theta_{max} = 4.018 + 1.0116\, T_{max} \quad \text{(A-6)}$$

Similarly, the relationships between minimum ambient air temperature and minimum mean bridge temperature and maximum ambient air temperature range and maximum mean bridge temperature range can be expressed as follows:

$$\theta_{min} = 6.1503 + 1.052\, T_{min} \quad \text{(A-7)}$$

$$\theta_{range} = -2.0225 + 1.0215\, T_{range} \quad \text{(A-8)}$$

where θ_{max}, θ_{min}, θ_{range} are the maximum, minimum, and range of mean bridge temperatures in $^{\circ}C$, and T_{max}, T_{min}, T_{range} are the maximum, minimum, and range of ambient air temperatures in $^{\circ}C$, respectively. The maximum ambient air temperature range is the difference between the maximum ambient air temperature in summer and the minimum temperature in winter at each station. Similarly, the maximum mean bridge temperature range is the difference between the maximum mean bridge temperature in summer and the minimum temperature in winter.

Demars [9] included a comparison of ranges based on the British code (BS5400) and ranges obtained by Moorty's equations. Because of England's mild climate, the BS5400 values were derived from a much smaller range of air temperatures. For a better result, Demars [9] used the same temperature values as those used for the BS5400 code to compare the two plots. The BS5400 values and the values obtained using Moorty's equations differed by a value of $5^{\circ}F$ or less for the maximum mean bridge temperature. The graph of minimum mean bridge values showed that Moorty's equations predicted higher temperatures in general, and the differences increased as the ambient air temperature increased. The maximum difference was approximately $9.5^{\circ}F$. The study

also revealed that both methods predicted composite mean bridge temperatures warmer than the surrounding air temperatures.

A comparison of the mean bridge temperature ranges obtained with Moorty's equation for the eleven stations across the United States and the ranges specified by AASHTO, 66.7°C to 83.3°C (120°F to 150°F) [1], indicates that almost all of the values except one are below the recommended code ranges. Therefore, the AASHTO specification over-predicts the movements for composite bridges in most areas. This suggests that better temperature ranges for the State of Washington need to be included in the design of bridges. An analysis of the temperatures at 49 different across the State of Washington was performed. The mean bridge temperature ranges for composite bridges were obtained using Moorty's equations. For greater accuracy, the equations derived from Moorty's method should be verified by taking a large number of data points.

APPENDIX B

AIR AND BRIDGE TEMPERATURES FOR 49 STATIONS IN WASHINGTON STATE

Table B-1. Air and Mean Bridge Temperature Values for 49 Stations

STATION	Longitu	Latitud	Elv.(m	Air Temperature, °C			Bridge Temperature, °C		
				Max.	Min.	Range	Max.	Min.	Range
Aberdeen	123.82	46.97	3	41	-14	55	45	-9	54
Anacortes	122.62	48.52	9	35	-16	51	39	-10	50
Bickleton	120.30	46.00	915	39	-27	66	43	-22	66
Buckley 1 NE	122.00	47.17	210	39	-19	59	44	-14	58
Cedar Lake	121.73	47.42	476	38	-24	62	43	-19	62
Centralia	122.95	46.72	58	40	-18	58	44	-13	57
Chelan	120.03	47.83	342	41	-28	69	46	-23	69
Clearbrook	122.33	48.97	18	39	-20	59	43	-15	58
Cle Elum	120.95	47.18	589	41	-36	77	45	-32	77
Colfax 1 NW	117.38	46.88	598	42	-36	78	47	-32	79
Colville AP	117.88	48.55	576	42	-36	78	46	-32	78
Concrete ppl Fish stn.	121.77	48.55	61	39	-18	57	43	-13	56
Cushman dam	123.22	47.42	232	40	-19	59	44	-14	58
Darrington R S	121.60	48.25	168	41	-26	66	45	-21	66
Dayton 1 WSW	118.00	46.32	476	46	-32	77	50	-27	77
Diablo Dam	121.15	48.72	271	41	-23	64	46	-18	64
Ellensburg	120.55	46.97	451	43	-35	78	48	-31	79
Ephrata Faa AP	119.52	47.32	384	46	-31	77	51	-27	77
Forks 1 E	124.37	47.95	107	39	-16	54	43	-10	54
Goldendale	120.83	45.75	503	42	-33	75	46	-29	75
La crosse	117.88	46.82	451	45	-37	82	50	-32	82
Landsburg	121.97	47.38	165	39	-18	57	43	-13	56
Lind 3 NE	118.58	47.00	497	45	-32	77	50	-28	77
Longview	122.92	46.15	3	42	-17	59	47	-12	59
Nespelem 2 S	118.98	48.13	576	43	-36	79	48	-32	80
Newport	117.05	48.18	653	42	-41	82	46	-37	83
Northport	117.78	48.92	403	43	-33	77	48	-29	77
Olga 2 SE	122.80	48.62	24	33	-22	56	38	-17	55
Olympia	122.90	46.97	58	40	-22	62	44	-17	62
Omak 2 NW	119.53	48.43	375	43	-32	75	47	-28	75
Palmer 3 ESE	121.85	47.30	281	38	-19	58	43	-14	57
Prosser 4 NE	119.75	46.25	275	43	-29	72	48	-24	72
Puyallup 2w Exp Stn	122.33	47.20	15	38	-19	58	43	-14	57
Quillayute	124.55	47.95	55	37	-15	52	42	-10	51
Rainier Paradise R S	121.73	46.78	1656	32	-28	59	36	-23	59
Seattle Tac wscmo AP	122.30	47.45	137	37	-14	52	42	-9	51
Sedro Woolley	122.23	48.50	18	36	-19	55	41	-14	54
Sequim	123.10	48.08	55	37	-19	57	42	-14	56
Snoqualmie Falls	121.85	47.55	134	39	-19	58	43	-14	58
Spokane wso AP	117.53	47.63	720	42	-32	74	47	-27	74
Stampede Pass	121.33	47.28	1208	33	-29	62	37	-25	62
Stehekin 4 NW	120.72	48.35	387	41	-29	70	45	-25	70
Vancouver 4 NNE	122.65	45.68	64	41	-23	64	45	-18	63
Walla Walla	118.40	46.05	244	43	-25	68	48	-20	68
Waterville	120.07	47.65	799	40	-36	76	44	-32	76
Wenatchee	120.32	47.42	195	43	-28	72	48	-24	72
Wilbur	118.67	47.75	680	43	-34	78	48	-30	78
Winthrop 1 WSW	120.18	48.47	537	41	-44	86	46	-41	86
Yakima	120.53	46.57	323	43	-32	75	48	-27	75

Table B-2. Air and Bridge Temperature Values Adjusted to Zero Elevation

STATION	Longit	Latitu	Elv.(n	Air Temperature, °C			Adj. Air Temp, °C			Adj. Br.
				Max.	Min.	Range	Max.	Min.	Range	Range,°C
Aberdeen	123.82	46.97	3	41	-14	55	41	-14	55	54
Anacortes	122.62	48.52	9	35	-16	51	35	-15	50	49
Bickleton	120.30	46.00	915	39	-27	66	38	-12	49	48
Buckley 1 NE	122.00	47.17	210	39	-19	59	37	-12	49	49
Cedar Lake	121.73	47.42	476	38	-24	62	33	-7	41	40
Centralia	122.95	46.72	58	40	-18	58	39	-16	55	54
Chelan	120.03	47.83	342	41	-28	69	37	-16	54	53
Clearbrook	122.33	48.97	18	39	-20	59	39	-19	58	57
Cle Elum	120.95	47.18	589	41	-36	77	36	-18	54	53
Colfax 1 NW	117.38	46.88	598	42	-36	78	38	-18	55	55
Colville AP	117.88	48.55	576	42	-36	78	37	-18	55	54
Concrete ppl Fish str	121.77	48.55	61	39	-18	57	38	-16	54	53
Cushman dam	123.22	47.42	232	40	-19	59	37	-11	49	48
Darrington R S	121.60	48.25	168	41	-26	66	39	-20	59	58
Dayton 1 WSW	118.00	46.32	476	46	-32	77	40	-15	56	55
Diablo Dam	121.15	48.72	271	41	-23	64	38	-14	52	51
Ellensburg	120.55	46.97	451	43	-35	78	38	-19	58	57
Ephrata Faa AP	119.52	47.32	384	46	-31	77	42	-18	60	59
Forks 1 E	124.37	47.95	107	39	-16	54	38	-12	50	49
Goldendale	120.83	45.75	503	42	-33	75	36	-16	53	52
La crosse	117.88	46.82	451	45	-37	82	40	-21	61	61
Landsburg	121.97	47.38	165	39	-18	57	37	-12	49	48
Lind 3 NE	118.58	47.00	497	45	-32	77	39	-15	55	54
Longview	122.92	46.15	3	42	-17	59	42	-17	59	59
Nespelem 2 S	118.98	48.13	576	43	-36	79	39	-18	56	55
Newport	117.05	48.18	653	42	-41	82	38	-23	60	60
Northport	117.78	48.92	403	43	-33	77	39	-19	59	58
Olga 2 SE	122.80	48.62	24	33	-22	56	33	-21	54	54
Olympia	122.90	46.97	58	40	-22	62	39	-20	60	59
Omak 2 NW	119.53	48.43	375	43	-32	75	38	-19	58	57
Palmer 3 ESE	121.85	47.30	281	38	-19	58	35	-10	45	44
Prosser 4 NE	119.75	46.25	275	43	-29	72	40	-19	60	59
Puyallup 2w Exp Stn	122.33	47.20	15	38	-19	58	38	-19	57	56
Quillayute	124.55	47.95	55	37	-15	52	37	-13	50	49
Rainier Paradise R S	121.73	46.78	1656	32	-28	59	39	-18	57	56
Seattle Tac wscmo A	122.30	47.45	137	37	-14	52	36	-10	46	44
Sedro Woolley	122.23	48.50	18	36	-19	55	36	-18	54	53
Sequim	123.10	48.08	55	37	-19	57	37	-18	54	53
Snoqualmie Falls	121.85	47.55	134	39	-19	58	37	-15	52	51
Spokane wso AP	117.53	47.63	720	42	-32	74	39	-15	53	53
Stampede Pass	121.33	47.28	1208	33	-29	62	35	-16	51	50
Stehekin 4 NW	120.72	48.35	387	41	-29	70	36	-16	53	52
Vancouver 4 NNE	122.65	45.68	64	41	-23	64	40	-21	61	60
Walla Walla	118.40	46.05	244	43	-25	68	41	-17	57	57
Waterville	120.07	47.65	799	40	-36	76	38	-20	57	56
Wenatchee	120.32	47.42	195	43	-28	72	41	-22	63	62
Wilbur	118.67	47.75	680	43	-34	78	40	-17	57	56
Winthrop 1 WSW	120.18	48.47	537	41	-44	86	36	-26	62	61
Yakima	120.53	46.57	323	43	-32	75	40	-21	61	60